Bioprinting 24 (2021) e00166

Contents lists available at ScienceDirect

Bioprinting

journal homepage: www.sciencedirect.com/journal/bioprinting

3D-printable conductive materials for tissue engineering and biomedical applications

Jiarui Zhou [a,b], Sanjairaj Vijayavenkataraman [a,b,*]

[a] The Vijay Lab, Division of Engineering, New York University Abu Dhabi, United Arab Emirates
[b] Department of Mechanical and Aerospace Engineering, Tandon School of Engineering, New York University, Brooklyn, NY 11201, USA

ARTICLE INFO

Keywords:
Conductive biomaterials
Bioprinting
Tissue engineering
Ionic liquids
Electrical stimulation

ABSTRACT

Many patients that undergo autografting suffer from donor site morbidity and risk of immune rejection. Tissue engineering is receiving considerable attention as engineered tissues could help overcome the drawbacks of autografts and achieve better performance on tissue repair, replacement and regeneration. Conductivity is one of the desired properties of engineered scaffolds and tissue constructs as bioelectricity plays an important role in the native physiological environment. Hence, conductive materials have been extensively used in the making of biosensors, tissue engineering scaffolds and drug delivery systems to elicit electrically-mediated signals, thus mimicking the natural cellular environment. Conductive polymers, carbon-based materials, and metal nanoparticles are the main categories of conductive materials used. Ionic liquids, especially biocompatible ionic liquids, is currently being explored as a competitive filler composite to greatly improve the conductivity of polymers with little to zero cytotoxicity. The effects of electrical stimulation on cell alignment, migration, proliferation, and differentiation as well as detailed properties of different types of conductive materials are briefly yet succinctly reviewed. Furthermore, 3D printing of conductive scaffolds and hydrogels, and their corresponding biomedical applications are also discussed.

1. Introduction

Tissue engineering, a rapidly progressing field, has the potential to meet the ever-growing demand for tissue and organ transplant, and to massively accelerate the development of new drugs and medications [1]. For many tissue engineering treatment methods, the gold standards have been well established. For example, connecting the nerve gap using autologous superficial cutaneous nerves has been considered the gold standard for the treatment of injured nerves [2]. However, due to the inherent limitation of autografts, such as donor site morbidity, donor site availability, and the creation of a second surgical site, tissue engineering has been emphasized as a novel treatment to deal with tissue and organ repair [2,3]. Stem cell therapy, as one of the tissue engineering strategies, might be able to achieve a full-scale tissue through the stem cell differentiation de novo from a patient's own stem cells [4]. Furthermore, it can eliminate the drawbacks of autografts and allografts, including lack of organ donors and life-long immunosuppression [5]. However, there are still several key factors that need careful consideration before engineered tissues could be transplanted *in vivo*, such as toxicity of the synthesized material, biodegradability and associated immune response.

As one of the promising materials used in the tissue engineering area, conductive polymers are synthetic polymers that conduct electricity [6]. It is also called intrinsically conducting polymers, which includes poly (3,4-ethylene dioxythiophene) (PEDOT): polystyrene sulfonate (PSS), Polyaniline (PANI), Polypyrrole (PPY), polythiophene and polyphenylene sulfide [2,7]. Recently, a lot of works have been devoted to developing high conductivity conductive polymers with the incorporation of carbon-based composites (carbon nanotubes, graphene oxide), metal nanoparticles (platinum, gold) and bio-ionic liquids [8–11]. Among the various biomedical applications, conductive polymers play an important role in electro-sensitive tissues such as muscle and nerve according to their excellent conductivity performance, which can provide electrical stimulation and mimic the physiological environment of the tissue [12]. Electrical stimulation could guide the stem cell to differentiate into a wide variety of specific cell types [13]. Particularly in neural tissue engineering, moderate electrical stimulation can accelerate the axonal growth of neurons, which would reduce the time required to bridge the nerve gap [14]. Tunable mechanical properties, simple synthesis process, high conductivity of conductive polymers makes it

* Corresponding author. Division of Engineering, New York University, Abu Dhabi, United Arab Emirates.
E-mail address: vs89@nyu.edu (S. Vijayavenkataraman).

https://doi.org/10.1016/j.bprint.2021.e00166
Received 28 March 2021; Received in revised form 4 August 2021; Accepted 9 August 2021
Available online 18 August 2021

available to be applied to various tissue engineering and biomedical applications [6]. Some of the common biomedical applications include biosensors, electrically induced drug release and delivery systems, and tissue engineering scaffolds [15,16].

While conductive materials address one aspect of biomimicry, there are other basic aspects of biomimicry in replicating the native tissue architecture. Considering the complex structure of native tissues and organs, 3D bioprinting is a promising technology to fabricate biomimetic structures. 3D bioprinting is a process of fabricating cell-laden bioinks into functional tissue constructs and organs from 3D digital models [3]. Unlike the conventional approaches, it provides high repeatability and flexibility by allowing a layer-by-layer construction of the 3D model [17]. The key properties of bioinks to be emphasized are different for various 3D bioprinting methods, for example, the viscosity of the synthesized material for inkjet bioprinting and photocurable materials for stereolithography [18,19]. Given the outstanding benefits of 3D bioprinting, it has a huge potential to be applied to tissue engineering and regenerative medicine.

The effects of electrical stimulation on cell alignment, migration, proliferation, and differentiation are briefly reviewed. The mechanical properties, conductivity, biocompatibility, biodegradability as well as synthesis process of conductive biomaterials, including conductive polymers, carbon-based materials, metal nanocomposites, ionic liquids and composites of synthesized conductive polymers with ionic liquids, and their applications in the area of tissue engineering are reviewed in detail. Furthermore, the 3D printability and 3D printing approaches for fabrication of conductive biomaterials are discussed which would overcome the limitations of conventional conductive substrate fabrication methods and achieve better efficiency as well as performance. At last, biomedical applications of 3D-printed conductive materials including both tissue engineering and biosensors are discussed (Fig. 1).

2. Electrical stimulation in tissue engineering

Tissue engineering, as a discipline of biomedical engineering, is a rapidly developing area integrating biology with engineering to achieve tissue repair, replacement and regeneration [20]. Especially in the tissue regeneration process, the use of autologous cells and stem cells to repair the damaged tissue is of particular importance [21,22]. It is known that cell growth status is directly linked to the performance of tissue regeneration. Electrical stimulation, as a method of physical stimulation, shows impressive potential to promote and regulate cell growth performance through activating intracellular signaling pathways and changing intracellular microenvironments [23]. Proper electrical stimulations can regulate the cell behavior and induce cell alignment, cell migration, cell proliferation, and cell differentiation, benefitting the tissue regeneration process (Fig. 2), while negligible and excessive electrical stimulations either has no effect or lead to cell death respectively [24]. Both electrical stimulation intensity and time need to be carefully optimized for inducing the desired effect. Besides, even the same electrical stimulation parameters can have different effects on different cell behaviors. For example, an electrical stimulation intensity less than 10 V/cm lead to better cell alignment, between 0.1 V/cm and 12 V/cm to maintain the cell viability and cell phenotype for cell migration and an intensity below 2 V/cm for extended time period (more than 7 days) for specific cell differentiation [23].

2.1. Electrical stimulation and cell alignment

Electrical stimulation has an interesting effect on decreasing the difference of cell angles, and redirecting the cell alignment to be consistent with the direction of electrical stimulation [25]. Electrical stimulation induces rearrangement of cytoskeleton, leading to changes in the cellular alignment/realignment. The direction of the cell alignment would be either perpendicular or parallel to the electrical field, depending on the type of cells [26,27]. Perpendicular alignment can minimize the voltage drop across a single cell by minimizing the transverse distance of electric field passing through it, while parallel alignment leads to interesting observations such as changing cell morphology for better alignment [2,28]. Yang et al. reported that rat adipose-tissue-derived stromal cells (ADSCs) maintained cell viability over 80% with a perpendicular alignment in both 2D culture (under a 6 V/cm electric field) and 3D culture (in a 3D collagen hydrogel) [29]. Zhao et al. cultured mouse fetal lung mesenchyme-4 (MFLM-4) cells in a direct current electric field [30]. The long axes of MFLM-4 cells were aligned perpendicular to the electric field vector, and the alignment performance continuously increased when the electric field intensity was increased from 150 to 400 mV/mm. Proper electric field intensity can promote the cell alignment, while excessive electric field intensity can lead to negative impact on both cell alignment performance and cell viability [31].

2.2. Electrical stimulation and cell migration

Electrical stimulation can regulate the direction and rate of cell migration through an inherent cell property called ‘electrotaxis’ [32]. On applying the electrical stimulation on cell-seeded scaffolds, there would be a directional electrical field pointing from cathode to anode,

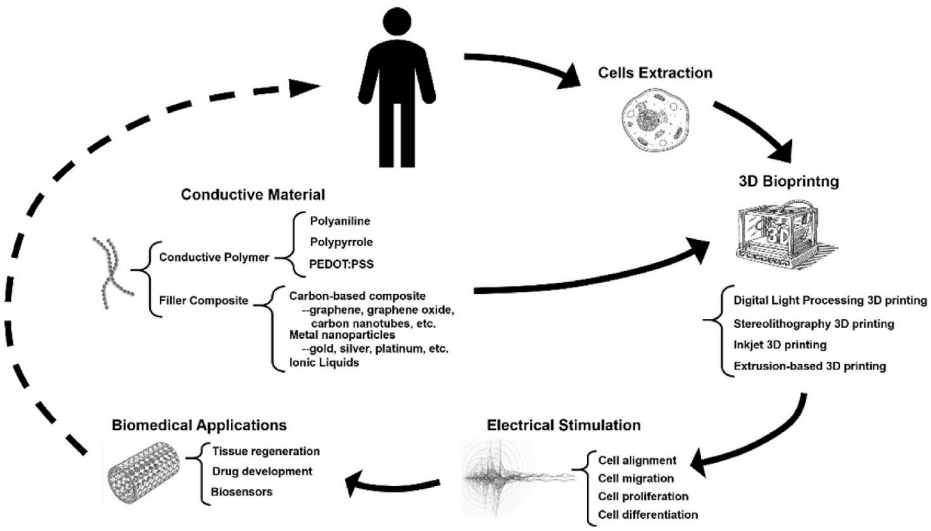

Fig. 1. 3D-printable conductive materials for tissue engineering applications.

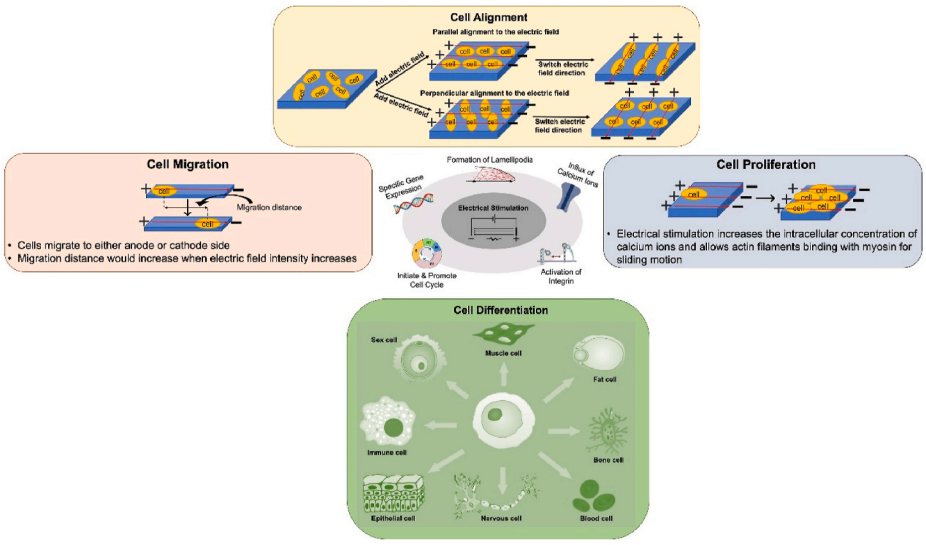

Fig. 2. Appropriate electrical stimulation can regulate cell alignment, cell migration, cell proliferation and cell differentiation.

which is considered as the direction of electrical stimulation or electric field direction. Cells can be divided into two types based on the electrotaxis phenomenon. One type of cells moves towards the cathode, including neural stem cells and neural precursor cells, and the other type of cells move towards anode, including human induced pluripotent stem cells (hiPSCs), Schwann cells, etc [33–36].

Cell migration, also known as cell crawling, happens in three steps: extension of leading edge, adhesion formation and retraction of rear edge (Fig. 3) [37]. Extension of leading edge is mainly achieved by the formation of lamellipodia and filopodia and both of those two structures are polymerized by the actin filaments and act as one type of network of actin filament. Adhesion formation is led by the activation of integrin, which is a transmembrane receptor connecting the extracellular matrix and intracellular cytoskeleton. Formation of focal adhesion allows the cell to closely attach on the substrate for the forward movement. Retraction of the rear edge is finished by the contraction between actin filaments and myosin filaments. Electrical stimulation activates both ERK1/2 and PI3K signal pathways [23]. Furthermore, Ca^{2+} ion channel is opened by the external electrical stimulation [38]. The cascading signal transduction of PI3K pathway could activate the unfolding of integrin and initiate the actin polymerization. ERK1/2 pathway could activate the expression of Arp2/3 (an actin nucleator) and then initiate the action polymerization. Activation of Ca^{2+} ion channel could lead to the influx of calcium ions, and the increasing concentration of calcium ions could phosphorylate the regulatory light chain of myosin filaments, promoting the contraction force generated by the combination between actin filaments and myosin filaments. Cumulatively, the activation of signal pathways and ion channels contributes to each step of cell migration, leading to the cell movement. Fig. 3 summarizes how electrical stimulation affects cell migration on each step.

Different human stem cells can exhibit completely different elextrotaxis. Feng et al. demonstrated that hiPSCs migrate to anode, while human embryonic stem cells (hESCs) migrate to the cathode [33,39]. Yao et al. reported that rat hippocampal neurons moved towards the cathode with an electrical stimulation. The net cell migration distance increased linearly with the increasing electric field intensity from 0 to 300 mV/mm, and the direction of cell migration was reversed on switching the polarity (Fig. 4), proving a clear cathodal migration of the neurons [40].

2.3. *Electrical stimulation and cell proliferation*

Proper electrical stimulation can accelerate cell proliferation to supplement the lost tissue structure during an injury process [23,41]. Electrical stimulation helps the transduction of proliferative signals by upregulating the cell nuclear antigen and activating the extracellular signal-regulated kinase 1/2 (ERK1/2) [23]. ERK1/2 plays a key role in regulating various processes, including metabolism, motility and cell viability, which are directly related to cell proliferation [42]. Myc gene and cyclin D are two products within the downstream ERK1/2 pathway, playing an important role in separating the combination of E2 Transcription Factor (E2F) and retinoblastoma protein (Rb), leading to the release and expression of E2F to initiate the cell cycle from G1 phase [43]. Durgam et al. compared the effect of electrical stimulation on cell

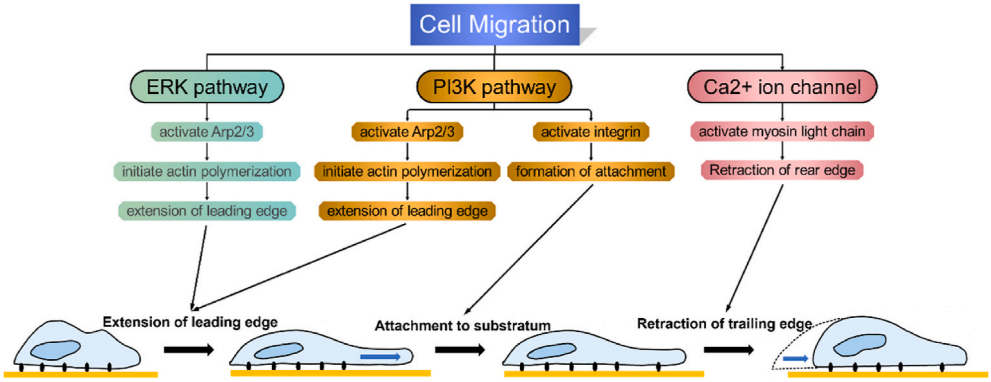

Fig. 3. Effect of electrical stimulation on cell migration: extension of leading edge, attachment to the substratum and retraction of trailing edge.

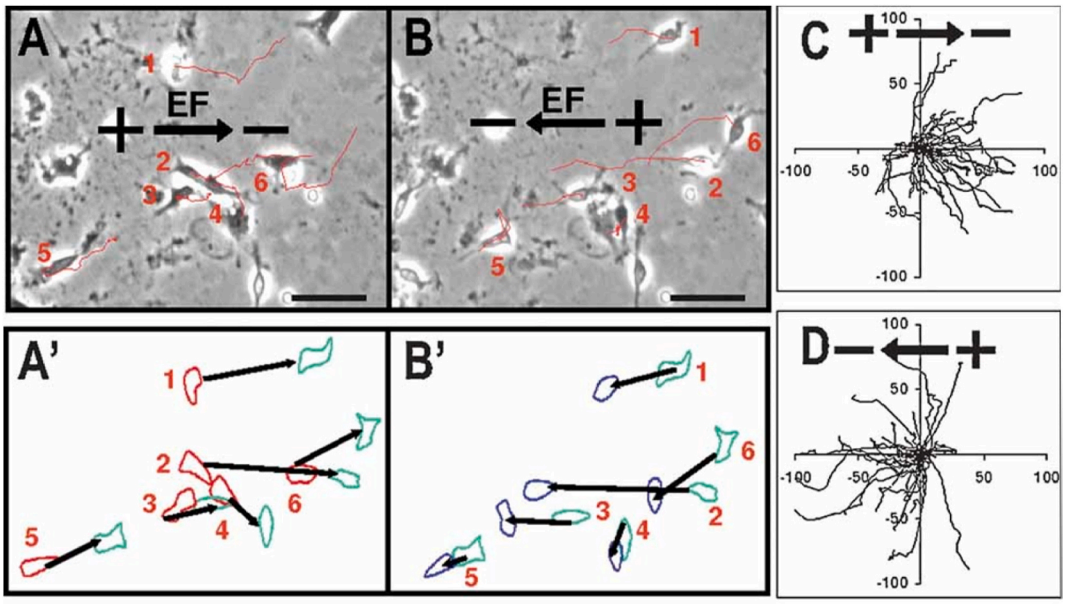

Fig. 4. Reversal of neuronal migration by providing another opposite direction electric field. (A) Trajectories of neuron migration (start from the end with numbers). All tracks belong to cathodal migration. (B) reversed migration trajectories of the same neurons in an opposite direction electric field (300 mV/mm). The outlines of the cells at the beginning and distal end of each migration trajectory with directions are indicated by red lines. A′, B': Outlines of the labeled cells from (A,B) highlight the trajectories of cell migration. C, D: Trajectories of neuron migration before and after the reversal of electric field. After reversing the electric field, neurons switched direction to migrate to the 'new' cathode. Scale bar: 50 μm [40]. (For interpretation of the references to color in this figure legend, the reader is referred to the Web version of this article.)

proliferation on a biodegradable polypyrrole/poly(ε-caprolactone) (PPy/PCL) conductive substrate for nerve regeneration applications [44]. The number of PC12 cells in PPy/PCL was found to be significantly increased with proper electrical stimulation compared to PPy/PCL without stimulation, which proves the effect of electrical stimulation on enhancing cell proliferation. Sun et al. showed that electrical

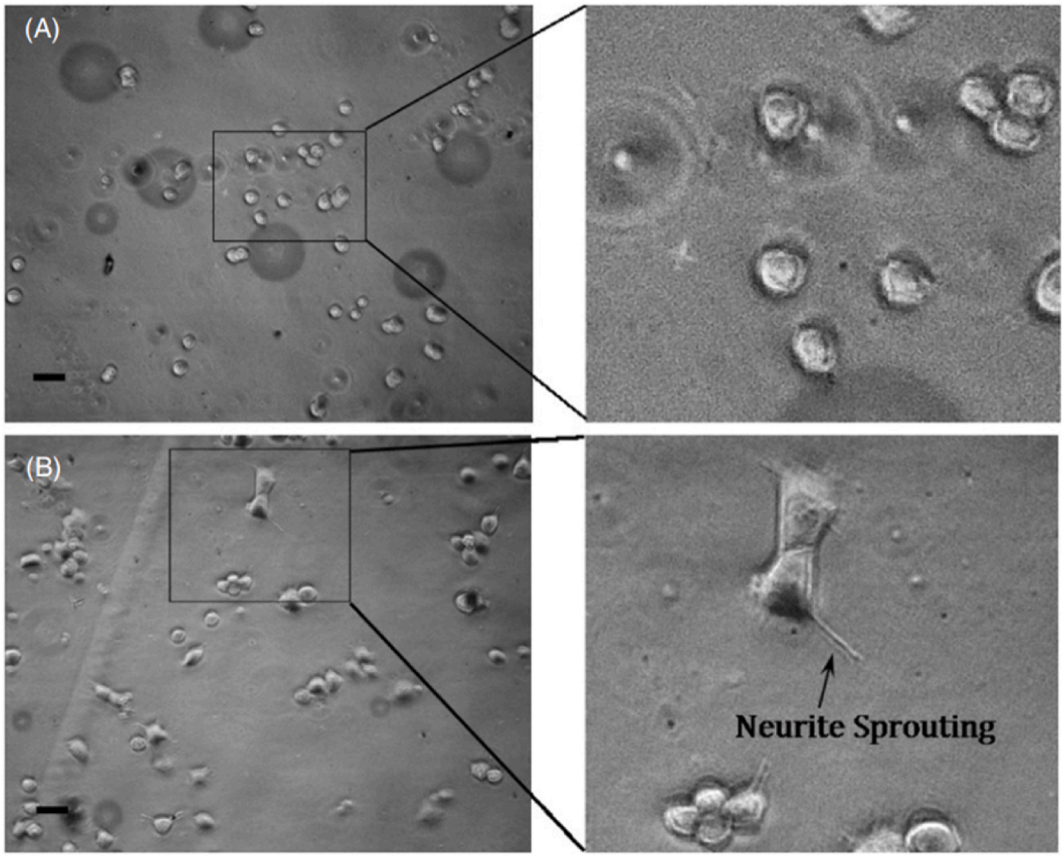

Fig. 5. Phase-contrast images of PC 12 cells on PPY/PMAS films without (A) and with (B) electrical stimulation in the absence of NGF. Scale bar: 20 μm [48].

stimulation can be used to promote proliferation of schwann cells without changing the cell morphology, which further indicates the potential applications of electrical stimulation on peripheral nerve repair and regeneration [45].

2.4. Electrical stimulation and cell differentiation

Cell differentiation is the process in which a cell changes its function or phenotype [46]. External electrical stimulation can lead stem cells to differentiate into specific cell types and promote the tissue regeneration process. Pires et al. demonstrated that human neural stem cells (hNSCs) experience an accelerated cell differentiation process under electrical stimulation of 1 V/cm, lasting for 8 days [47]. The number of differentiated neurons from hNSCs were higher in the electrical stimulation group compared with no stimulation group. Furthermore, longer neurites are detected as well due to the positive effect of electrical stimulation. In the presence of nerve growth factor (NGF), Liu et al. showed a significant promotion of PC12 differentiation under a 250 Hz biphasic current pulses for 3 consecutive days [48]. The result indicates that electrical stimulation can significantly promote PC12 differentiation with the incorporation of NGF. While in the absence of NGF, they experienced a reversible neurite sprouting with and without electrical stimulation (Fig. 5), which makes NGF a vital component in the cell differentiation process. However, Sun et al. proved that electrical stimulation can promote PC12 cell differentiation without the presence of NGF [45]. The number of differentiated cells as well as axon length are significantly increased by enhancing the gene expression level of β-Tubulin III, GAP43, and synapsin I. Furthermore, the absence of NGF strongly reveals that electrical stimulation alone can promote the cell differentiation. Therefore, electrical stimulation is a promising method to promote peripheral nerve regeneration, with or without the presence of associated growth factors.

The effects of electrical stimulation on cell behavior are summarized in Table 1.

3. Conductive materials

Conductive materials used in the area of tissue engineering could be primarily classified into two groups: conductive polymers and conductive filler materials (carbon-based materials including graphene, metal nanoparticles, and ionic liquids). Conductive polymers, with wide ranges of electrical properties, can be synthesized using various simple and flexible methods [2]. Conductive polymers, being non-toxic and possessing excellent electrical properties, have been explored widely for various biomedical applications such as nerve conduits in neural tissue engineering, scaffolds for cell adhesion and proliferation, and various drug delivery and drug release systems [9,12,14,58,59]. Various types of fillers can be synthesized together to enhance the conductivity, apart from the primary conductivity brought by the inherently conductive polymers. The most commonly used fillers are carbon-based fillers, metal nanoparticles, and ionic liquid [8,10,11]. The conductivity of conductive polymers can also be dramatically increased by chemical or electrochemical processes, such as p-doping (oxidation) and n-doping (reduction) [60]. By using different types of dopants and levels of doping, conductive polymers exhibit a highly flexible tunability for electrical properties [61]. In this section, the mechanical properties and electrical performance of different conductive polymers and filler composites are discussed. A comprehensive overview of the classification of conductive materials is presented in Fig. 6.

3.1. Conductive polymers

Conductive polymers, also known as intrinsically conductive polymers, have a wide range of conductivity crossing several orders of magnitude, depending on the dopant types and doping levels. Conductive polymers have been extensively studied and applied in a large

Table 1
Effect of electrical stimulation on cell behavior.

Cell type	Electrical stimulation intensity	Effect on cell behavior	Ref.
Schwann cell	100 mV/cm for 1 h per day for 5 days	Cell proliferation with elongated and spreading morphology	[45]
PC12	100 mV/cm for 1 h per day for 5 days	Cell differentiation by significant increasing axon growth	[45]
Mesenchymal stem cell (MSC cell)	0.15 V/cm for 2 ms duration at a frequency of 1 Hz for 14 days	Cell alignment by reorienting the cell perpendicular to the direction of the current	[49]
Meniscus cell	3 V/cm for 2 ms pulse duration at a frequency of 1 Hz	Enhanced cell migration in both 2D and 3D test with no preference to a specific pole	[50]
Meniscus cell	0–6 V/cm with the best cell migration performance at 6 V/cm	Cell migration to the cathode direction when aligned perpendicular to the direction of the electric field	[51]
MFLM-4 cells	150 mV/mm to 400 mV/mm for 4 h	Cell alignment perpendicular to the vector of electric field	[30]
Schwann cell	Constant electric field at 500 mV/mm for 2 h	Cell alignment perpendicular to the vector of electric field. (mean angle of 69.9 ± 19.0°)	[31]
Myoblasts	–	Cell alignment parallel to the vector of electric field. (over 90% of fiber angles were reoriented within ±20°)	[52]
Myoblasts	2 V/cm DC electric field for 10 min and 20 min rest periodically	Enhanced cell differentiation by inducing myotube formation	[52]
Rat calvarial osteoblasts	Strong DC electric field at 10–15 V/cm and weak DC electric field lower than 5 V/cm	Cell migration to the cathode direction	[53]
Human SaOs-2 cells	Strong DC electric field at 10–15 V/cm and weak DC electric field lower than 5 V/cm	Cell migration to the anode direction	[53]
human neural progenitor cells	Pulsed electric field (1 Hz, 100 Hz, 1000 Hz) at 250 mV/mm for 6 h	Cell migration to the cathode direction with greater migration distance	[54]
Neural stem cells	–	Cell proliferation rate increased 35% compared to the cells without electrical stimulation	[55]
Neural stem cells	–	Enhanced cell differentiation. More neuronal differentiation marker MAP2 was expressed and observed	[55]
Cardiomyocytes	Direct 1 μA microcurrent over a period of 7.7 ± 0.9 h per day	Enhanced cell proliferation with more cell number compared to cells without microcurrent	[56]
PC12 cells	Constant current of 100 μA for 2 h	Enhanced cell proliferation with more cell numbers.	[44]
Human neural stem cells	1 V/cm for 8 days	Accelerated cell differentiation process	[47]
PC12 cells			[48]

(continued on next page)

Table 1 (*continued*)

Cell type	Electrical stimulation intensity	Effect on cell behavior	Ref.
Cardiac adipose tissue-derived stromal cells (ATDPCs) and Subcutaneous ATDPCs	250 Hz biphasic current pulses for 3 days monophasic square-wave pulses of 50 mV/cm at 1 Hz with an alternating current of 2 ms over 14 days	Enhanced cell differentiation with increasing neurit length Cell alignment by reorienting the cell perpendicular to the electric field	[57]

number of applications, including organic solar cells, rechargeable battery electrodes, supercapacitors, biosensors and tissue engineering areas [7,62–65]. Due to their outstanding electrical conductivity, biocompatibility and chemical stability, PPY, PANI and PEDOT:PSS are the three commonly used conductive polymers in tissue engineering and biomedical applications [66–68]. However, different conductive polymers have distinct inherent drawbacks, such as poor mechanical properties for PPY, and poor solubility and non-degradability for PANI, which would limit the use of these conductive polymers for biomedical applications [15]. Conductive polymers can be co-synthesized or co-polymerized with other polymers to impart the benefits of both components and overcome the inherent disadvantages of conductive polymers. Wu et al. developed a highly stretchable conductive N-acryloyl glycinamide-co-2-acrylamide-2-methylpropanesulfonic (PNAGA-PAMPS)/PEDOT:PSS hydrogel (Fig. 7) as a promising electro-active biomaterial for use in tissue engineering [69]. PEDOT: PSS increases the conductivity of the hydrogel composite and the range of conductivity achieved was 0.2 S/m to 2.2 S/m by increasing the doping percentage of PEDOT: PSS. Furthermore, *in vitro* cytotoxicity test showed a cell viability of 74–100%, proving that the developed hydrogel is non-cytotoxic and suitable to be applied for soft tissue engineering and biomedical applications. Wang et al. formulated a conductive hydrogel composed of PANI and poly(acrylamide-co-hydroxyethyl methyl acrylate) (P-(AAm-co-HEMA)) with a very low PANI threshold of 0.5 wt/vol % [70]. The conductivity of the composite hydrogel increases consistently by increasing the PANI content from 0.1 wt/vt% to 0.5 wt/vt%, which is the threshold concentration. The conductivity at threshold concentration was 8.24 ± 0.57 S/m, which is close to the conductivity of pure PANI (11 S/m).

Table 2 lists the properties of commonly used conductive polymers and metal nanoparticles.

3.2. Carbon based filler composites

There is a broad family of carbon-based composites, including activated carbon-based composites, ordered mesoporous carbon-based composites and carbon nanotube-based composites that are used as filler materials to enhance the conductivity of polymer or hydrogel composites [82]. However, considering the biocompatibility, processibility, electrical and mechanical properties, the commonly used carbon-based filler composites are limited to graphene and carbon nanotube-based composites. Tadyszak et al. present an overview on the structure of graphene-based composites (Fig. 8) [83].

Graphene has a high surface to volume area, great chemical stability, excellent electrical conductivity, and good mechanical properties, such as high tensile strength and elastic modulus [84–87]. Graphene-based composites such as graphene oxide, reduced graphene oxide, and partially reduced graphene oxide are extensively used as dopants to be mixed with conductive polymers to enhance the conductivity of the synthesized composites [88–90].

Compared with graphene, graphene oxide exhibits poor mechanical properties (elastic modulus and tensile strength) as well as lower electrical conductivity [85,86,91,92]. However, graphene oxide is highly hydrophilic due to the oxygen-containing functional groups, which makes the graphene oxide a perfect material for producing homogeneous aqueous suspensions [93,94]. Furthermore, graphene oxide is a biocompatible nanomaterial and has extensively been explored in tissue engineering and biomedical areas [95]. Xiao et al. introduces a novel polyvinyl alcohol (PVA)/polyethylene glycol (PEG)/graphene oxide hydrogel composited with nano-woven fabric to produce electrocardiogram (EDG) electrodes [9]. Both PVA and PEG have poor mechanical properties, therefore the addition of graphene oxide is an effective method to significantly improve the polymeric mechanical performance due to crosslinking between graphene oxide polar groups and polymeric branches [96]. Furthermore, the high surface to volume ratio of graphene oxide allows more active electron mobility, which reduces the electro-resistance of the hydrogel.

Reduced graphene oxide shows a higher electroactivity as well as mechanical strength compared to graphene oxide, which allows the fabrication of highly robust materials [6]. Furthermore, reduced graphene oxide has been evaluated to be stable in aqueous medium and biocompatible, which satisfies the criteria for many biomedical applications [97]. Shin et al. incorporated reduced graphene oxide into the gelatin methacryloyl (GelMA) matrix to produce a hybrid hydrogel [98]. The electrical impedance of the hybrid hydrogel decreased with

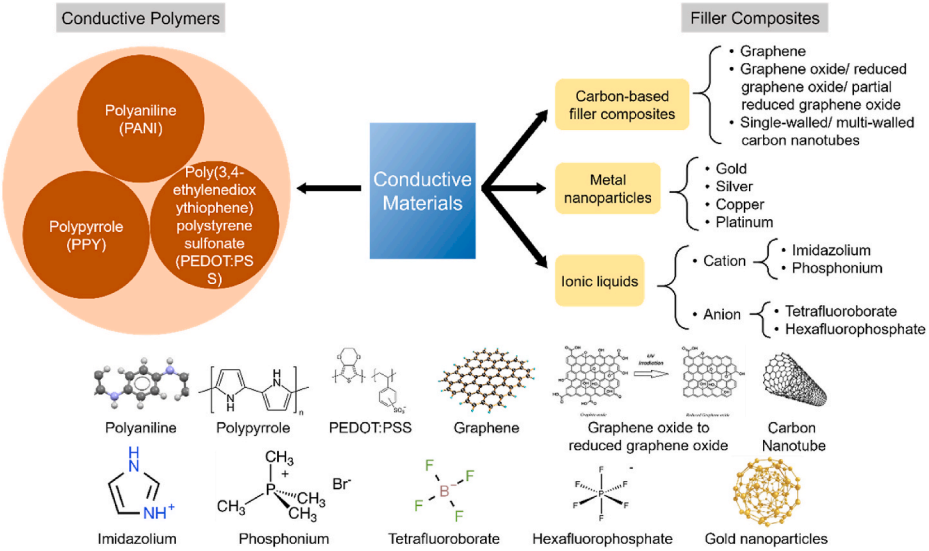

Fig. 6. Conductive materials for biomedical applications.

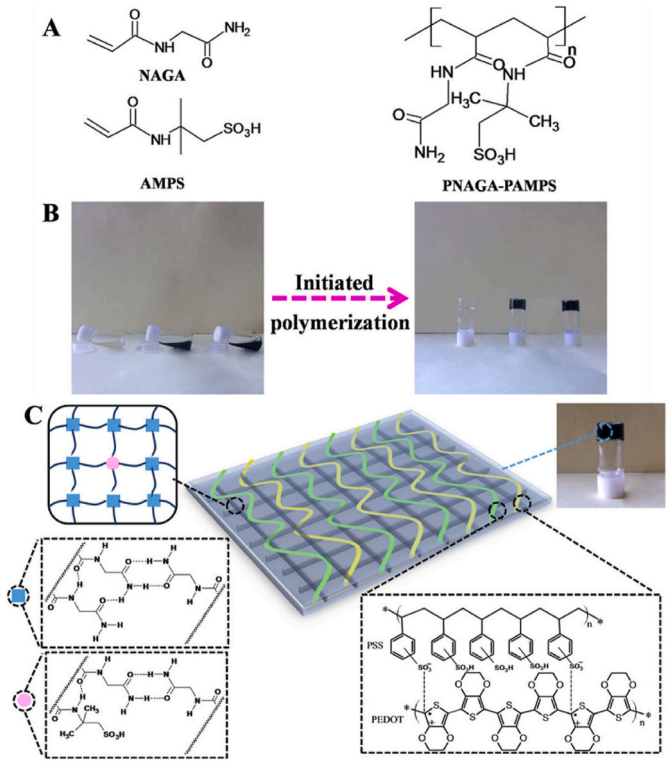

Fig. 7. (A) Schematic diagram of the molecular structures of N-acryloyl glycinamide (NAGA), 2-acrylamide- 2-methylpropanesulfonic acid (AMPS), and poly (NAGA-co-AMPS) (PNAGA-PAMPS). (B) Gelation process of aqueous solutions of PNAGA-PAMPS/PEDOT/PSS-X-49 (X equals 0, 3, 5 from left to right) (C) Schematic illustration of the synthesized network structures crosslinked by dual amide hydrogen bonds and doped with PEDOT: PSS [69].

increasing concentration of reduced graphene oxide (from 0 mg/ml to 5 mg/ml), demonstrating that the incorporation of reduced graphene oxide markedly enhances both the mechanical and electrical properties. The results demonstrate the cytocompatibility of hybrid hydrogel and a higher concentration of reduced graphene oxide could result in better initial homogeneous cell attachment and spreading. Apart from graphene oxide and reduced graphene oxide, partially reduced graphene oxide (graphene oxide is partially reduced to graphene by controlling the reaction time) had also been proved to possess excellent biocompatibility with no inflammatory reactions during *in vivo* and *in vitro* evaluations [90]. In addition, partially reduced graphene oxide has been shown to have better cell adhesion and proliferation compared to graphene oxide [98].

Carbon nanotubes (CNTs) are one-dimensional allotropes of carbon, which are formed by the hexagonal arrangement of different carbon atoms with a cylindrical structure [99,100]. To investigate how conductivity relies on the concentration of CNTs, Mottet et al. formulated a conductive composite hydrogel consisting of alginate and carbon nanotubes [101]. An electroanalytical method was used to assess the conductivity performance with varying concentrations of CNTs from 0 wt% to 2.5 wt%. It is found that the conductivity is almost zero at a low concentration of CNTs, while it shows a sharp increase beyond a critical concentration C^{C}_{CNT}, which is roughly 0.5 wt%.

3.3. Metal nanoparticles

Metal nanoparticles are solid nanoscale particles formed by pure metals or their compounds, which are produced by chemical or mechanical methods [102]. The most commonly used metal nanoparticles in tissue engineering and biomedical applications are silver and gold nanoparticles with a small proportion of platinum nanoparticles [103–105]. Different types of nanoparticles have their unique benefits, for example, silver nanoparticles have been extensively used as an antimicrobial agent, while owing to the advantages of biocompatibility, facile fabrication and modification process, gold nanoparticles have been treated as a promising material for bioimaging [106–108]. However, cytotoxicity has always been an issue with metal nanoparticles,

Table 2
Properties of commonly used conductive polymers and metal nanoparticles.

Materials	Tensile strength (MPa)	Young's Modulus (GPa)	Conductivity (S/cm)	Bio-related properties	Drawbacks	Ref.
Polypyrrole	40–50	1.4–2.25	100–7500	high electrical conductivity, biocompatibility, environmental stability, accelerate cell polarization rate, low subacute toxicity	brittle, insoluble, infusible, hard to process	[2,71–73]
Polyaniline	45–420	1.3 ± 0.2	30–200	high electrical conductivity, support cell adhesion and proliferation, excellent biocompatibility	brittle, lack of solubility	[2,72, 74–76]
PEDOT: PSS	25–55	1.0–2.7	Up to 4600 ± 100	water-soluble, biodegradable, biocompatible	acidity, anisotropic charge injection, batch-to-batch variation	[77–79]
Gold (Au)	–	–	5×10^5	–	–	[80]
Silver (Ag)	–	–	6.3×10^5	–	–	[81]
Copper (Cu)	–	–	6.0×10^5	–	–	[81]
Platinum (Pt)	–	–	1.0×10^5	–	–	[81]

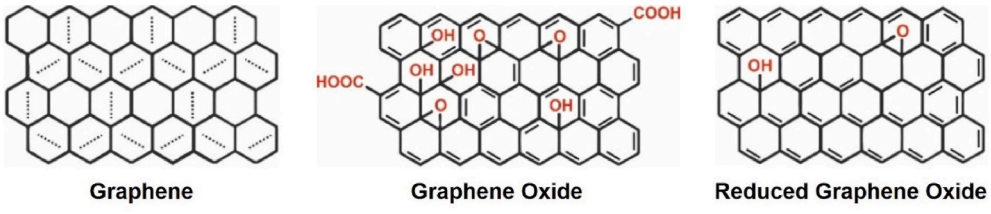

Fig. 8. Schematic illustration of molecular structures of graphene, graphene oxide (GO), and reduced graphene oxide (rGO) [83].

which has to be carefully examined before applying to tissue engineering applications. Baei et al. developed a thermosensitive chitosan based conductive hydrogel with evenly dispersed gold nanoparticles [10]. Different concentrations of gold nanoparticles/chitosan (0 %w/w, 0.5 % w/w, 1 %w/w and 1.5 %w/w) were tested. The conductivity of 1%w/w gold nanoparticles/chitosan is roughly 0.13 S/m, which is close to the conductivity of the physiological myocardium. Li et al. formulated a conductive polymer polyaniline hydrogel with a homogeneous high-density loading of platinum nanoparticles and developed a multiplex biosensor using the composite hydrogel as the working electrode material [109]. Owing to the high conductivity, good biocompatibility and excellent biosensing performance of the composite hydrogel, detection of triglyceride, lactate and glucose with high sensitivity was achieved.

3.4. Ionic liquids

Ionic liquids (ILs) are a class of organic salts composed only of ions [110]. ILs are being used as solvents and reaction media, and possess many advantages such as nonflammability, thermal stability, and near to zero vapor pressure [111,112]. Theoretically, by changing different cation and anion groups, more than 1 million ILs can be synthesized, providing a huge freedom to formulate unique ILs targeting specific applications [113]. However, many commonly used ILs exhibit cytotoxicity that limit their use in biomedical applications [113]. In order to fully expand the biomedical applications of ILs, reducing cytotoxicity is one of the most critical first steps.

Due to the presence of ionic components, ILs exhibit a wide range of electrolyte conductivity [114]. Therefore, ILs can be used as a potential candidate to increase the conductivity of both non-conductive and conductive polymers. Based on the different cation/anion components, there are various types of ILs such as choline-based ILs, and glycine-based ILs. Among various cation/anion components, using choline as cation moiety can provide the ILs with excellent biodegradability and low toxicity [115,116]. Noshadi et al. formulated a novel electroconductive hydrogel using non-conductive polymers and a choline-based bio-ionic liquid (Fig. 9A and B) [11]. Choline acrylate is used as the bio-ionic liquid, while gelatin methacryloyl (GelMA) and poly(ethylene glycol) diacrylate (PEGDA) are the two polymers used. The conductivity of both GelMA/ILs and PEGDA/ILs hydrogel increased with increasing IL concentration (Fig. 9C). Furthermore, both GelMA/ILs and PEGDA/ILs showed excellent degradation rate over a four-week period in the *in vitro* cell seeding experiment (Fig. 9E and F), with the degradation rate continuously increasing with the increasing ratio of ILs in the polymer/ILs composite. Comparing the cell behavior between pure GelMA (control group) and GelMA/ILs composite, cell viability (Fig. 9D), metabolic activity and cell numbers of GelMA/ILs composite are all higher than the pure GelMA group, proving the biocompatibility and non-toxicity of GelMA/ILs as well as choline acrylate.

Table 3 summarizes both mechanical, electrical and biological properties of different conductive materials.

4. 3D bioprinting

3D bioprinting as a process of directly fabricating cell-laden bioinks into functional tissue constructs and organs is increasingly becoming the mainstream technology in tissue engineering and regenerative medicine [3,120]. Similar to the conventional 3D printing methods, 3D bioprinting possesses a lot of advantages, including automation, high precision and a wide range of degrees of freedom on both design geometry and materials [3]. However, unlike conventional 3D printing method, besides rheological properties of materials, printing resolution, speed and accuracy, unique properties like post-printing cell viability become critical in the evaluation of suitable 3D bioprinting methods [121–123]. Light-based, inkjet, and extrusion bioprinting are the three most commonly used 3D bioprinting methods (Fig. 10A–D). Different methods have different key properties to be emphasized, for example, viscosity for inkjet bioprinting and UV light intensity for light-based bioprinting [124–126]. 3D printing of internal features requires additional supporting materials for both inkjet and extrusion bioprinting methods, leading to the demand of dual-nozzle system and therefore increasing the complexity and cost of the bioprinter. Furthermore, the removal process of supporting materials may cause a secondary damage on the mechanical properties of the structure. Owing to the advance of UV curing technology, fast transition time from liquid state to solid state is determined by the use of light-based bioprinter to realize a better structural integrity of internal features. However, the solid requirement of photosensitive material results in low selectivity of light-based bioprinting. The x-y resolution of inkjet and extrusion bioprinting is limited by the nozzle diameter and the diameter of commonly used commercial nozzle is 0.2 mm due to the tradeoff between viscosity and nozzle diameter, while the x-y resolution of light-based bioprinting is determined by the pixel resolution of the digital micromirror devices (as the process is nozzle free). Furthermore, not only the synthesized conductive materials can be 3D printed, even ionic liquids, which are performed as filler composites, can be 3D printed as well [127]. An overview of the advantages, disadvantages, applications of commonly used 3D bioprinting methods are presented in this paper.

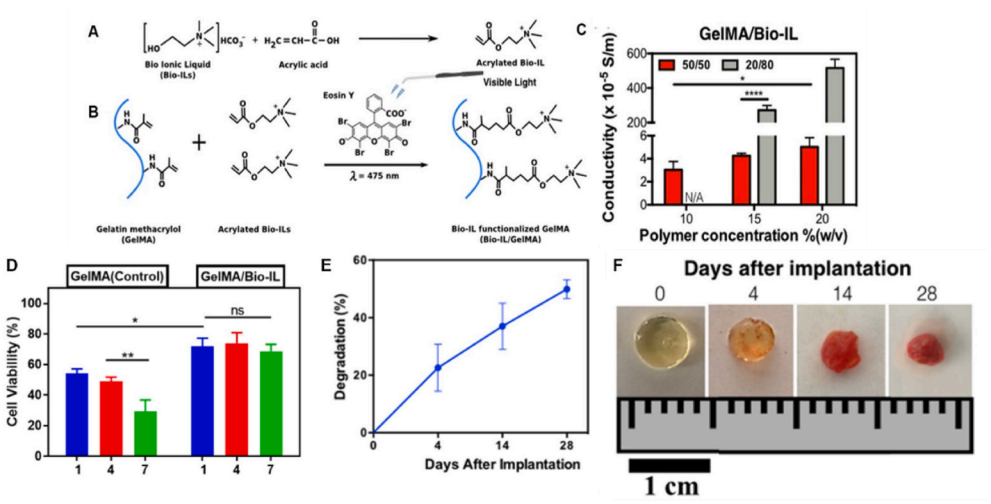

Fig. 9. Synthesis process and electrical property of Bio-IL incorporated GelMA hydrogels. (A) chemical reaction between choline bicarbonate and acrylic acid to form Bio-IL. (B) chemical reaction between GelMA and Bio-IL to form GelMA/Bio-IL hydrogel in the presence of Eosin Y and visible light. (C) Conductivities of GelMA hydrogels at different polymer concentrations %(w/v) and polymer/Bio-IL ratios. (D) Quantification of cell viability for 3D encapsulated CMs/CFs in both GelMA and GelMA/Bio-IL hydrogels on days 1, 4, and 7 post-encapsulations. (E, F) Evaluation of the post-implantation (*in vivo*) degradation status of GelMA/Bio-IL hydrogels on days 0, 4, 14 and 28 [11].

Table 3
Mechanical, electrical and biological properties of conductive materials.

Conductive material	Concentration	Mechanical properties	Conductivity (S/cm)	Biocompatibility	Ref.
PNAGA-PAMPS hydrogel with PEDOT/PSS	PEDOT/PSS concentration from 0% to 5% in the volume ratio of the dissolved mixture	Tensile strength 0.22–0.58 MPa, Young's modulus 30–110 KPa	2×10^{-3} to 2.2×10^{-2}	*In vitro* cytotoxicity test proves the conductive gels can maintain 74–100% cell viability	[69]
PANI with poly(acrylamide-co-hydroxyethyl methyl acrylate)	The threshold concentration of 0.5% of PANI in the volume ratio	Ultimate tensile strength 7.27 MPa	$(8.14 \pm 0.5) \times 10^{-2}$		[70]
PEG-DA with PEDOT:PSS	PEG-DA and PSS with 3:1 vol ratio	The compressive modulus of 21 KPa	1.69×10^{-2}	*In vitro* study uses H9C2 myocytes shows non-cytotoxicity, enhanced cell adhesion and proliferation	[12]
Gelatin methacrylate with gold nanorods	10 % w/v GelMA hydrogel woth 1 mg/ml gold nanorods		Decreased impedance compared to pure GelMA	Supports cardiac cells functionalities in a biomimetic fashion	[16]
PEG-DA with PEDOT:PSS and reduced graphene oxide	0.25% w/w rGO dopant and 10% w/v PEDOT:PSS	Elastic modulus is roughly 260 KPa	$(4 \pm 0.4) \times 10^{-3}$		[6]
Sodium alginate, carboxymethyl chitosan, PPY	The mass ratio of SA: CMCS is 2:1, PPY mass ratio is 0.4	Young's modulus 0.406 MPa, tensile strength 0.049 MPa, Porosity 62.87%, swelling ratio 5.013	8.03×10^{-3}	Used as a filling material for nerve conduit in the animal experiment and no obvious inflammation was observed	[14]
GelMA, PEDOT:PSS, PEG-DA	0.91% w/w PEDOT:PSS	Compressive modulus 26.3 ± 4.2 MPa	0.824×10^{-2} to 1.383×10^{-2} under 1 mm thickness film	Minimal cytotoxic effects and enhanced neural differentiation were observed when DRG cells were seeded into the hydrogel structure	[7]
PDA, partially reduced graphene oxide, PAM	Graphene oxide/AM 2 wt%, DA/AM 0.8 wt%	Tensile strength 62.5 KPa	0.08	Yield excellent signals from the dorsal muscle after implantation during an *in vivo* test	[90]
Polycaprolactone (PCL), reduced graphene oxide (rGO)	2.5 mg of rGO powder, 70% (w/v in acetic acid) PCL	yield strength 1.51 ± 0.3 MPa, ultimate stress 2.39 ± 0.3 MPa, Young's modulus 16.76 ± 3 MPa	$1.35 \pm 0.3 \times 10^{-3}$	*In vitro* test of PC12 cells presented better proliferation and neurite extension performance in PCL/rGO scaffolds	[117]
PPY, Polycaprolactone	block copolymer of PPy and Polycaprolactone (PPy-b-PCL) 0.5, 1 and 2% v/v	Young's modulus between 51 ± 4.55 MPa (PCL/PPy 0.5%) and 35 ± 5.6 MPa (PCL/PPy 2%)	2.8×10^{-4} to 1.15×10^{-3}	Human embryonic stem cell-derived neural crest stem cells (hESC-NCSCs) was capsulated in PCL/PPY (1%) scaffold and experienced enhanced proliferation and differentiation to peripheral neuronal cells	[118]
chitosan (CS), Gold nanoparticles (GNPs)	GNP/CS (% w/w) = 1.0		1.3×10^{-3}	Mesenchymal stem cells were cultured in the *in vitro* test and maintained the metabolism and proliferation	[10]
PEDOT: PSS, carbon nanotube (CNT) fibers	PEDOT: PSS = 1:1.08		58.6		[58]
polyacrylate, graphite micropowder	0.1 wt% crosslinker, 1.5 wt% initiator, 75% neutralization degree, 5 wt% graphite, 50 wt% monomer concentration and a reaction temperature of 80 °C		7.3×10^{-3}		[119]
oligo (poly (ethylene glycol) fumarate) (OPF) with positive charges, graphene oxide acrylate (GOa), carbon nanotube poly-(ethylene glycol) acrylate (CNTpega), 2-(methacryloyloxy) ethyltrimethylammonium chloride (MTAC)		swelling ratio 8.7 ± 0.5, compressive mudulus 850.5 ± 670.5 kPa	$(5.75 \pm 3.23) \times 10^{-5}$	Enhanced proliferation of encapsulated PC12 cells. A good material for nerve guide conduits fabrication	[8]
PANI, platinum nanoparticles				Used as biosensor to detect triglyceride, lactate, glucose	[109]
PEGDA, bio-ionic liquid (choline bicarbonate and acrylic acid)	Polymer/bio-ionic liquid ratio: 100/0 (control), 80/20, 50/50, and 20/80	Elastic moduli: 2.60 ± 0.46 kPa to 172.70 ± 2.86 kPa	$1{,}262 \times 10^{-7} \pm 420 \times 10^{-7}$		[11]
GelMA, bio-ionic liquid (choline bicarbonate and acrylic acid)	Polymer/bio-ionic liquid ratio: 100/0 (control), 80/20, 50/50, and 20/80	Elastic moduli: 5.20 ± 1.15 kPa to 100.77 ± 23.95 kPa	$516 \times 10^{-7} \pm 50 \times 10^{-7}$ (maximum)	Biodegradable and biocompatible. Better cell viability under 3D encapsulation of cardiomyocytes and cardiac fibroblasts than pure GelMA	[11]
PPY, poly(ε-caprolactone) (PCL)			32	PC12 cells were seeded on the film for *in vitro* test. Excellent conductivity of the film enhanced cell proliferation and cell differentiation of PC12 cells	[44]

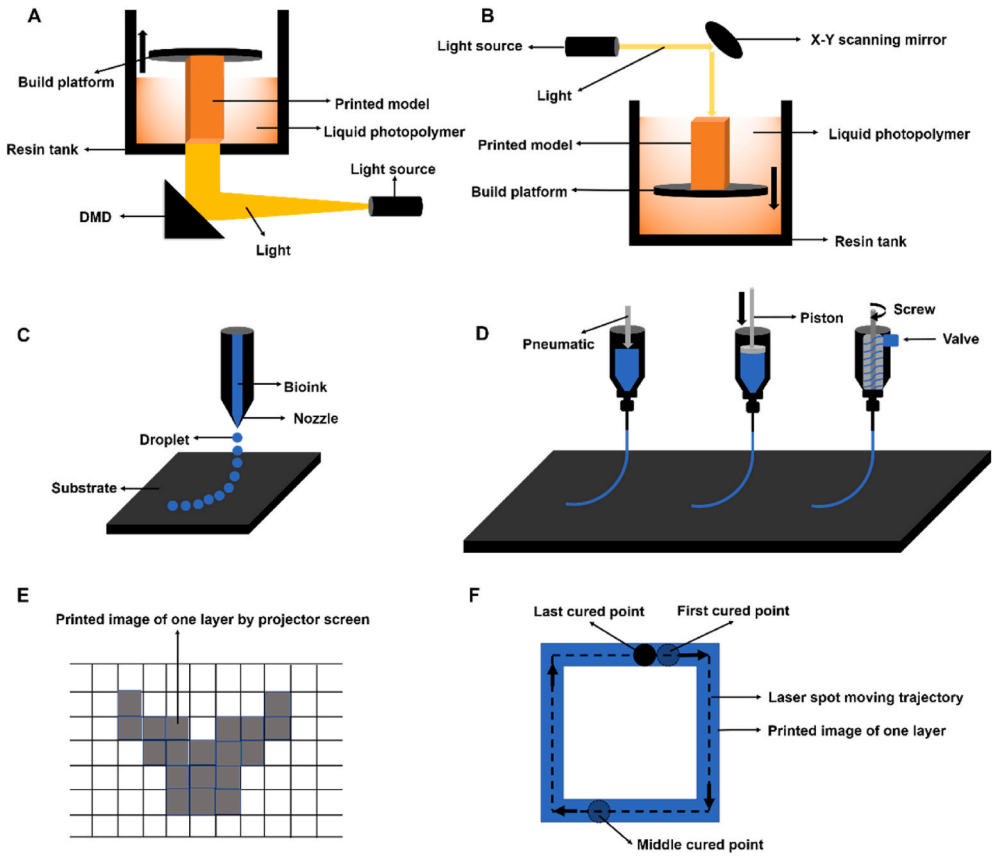

Fig. 10. Most commonly used 3D bioprinting methods in tissue engineering and biomedical area. (A) Digital light processing 3D printing. (B) Stereolithography 3D printing. (C) Inkjet Bioprinting. (D) Micro-extrusion bioprinting. (E) Digital light processing 3D printing method of one layer. (F) Stereolithography 3D printing method of one layer.

4.1. Light-based bioprinting

Light-based bioprinting is based on the photopolymerization property of printed materials [128]. Exposure to a UV light or laser or visible light layer-by-layer or voxel-by-voxel induces photopolymerization and crosslinking of the resin, thus forming the 3D object. Two frequently used light-based bioprinting methods are digital light processing (DLP) 3D printing and stereolithography (SLA) 3D printing. One of the primary differences between these two methods is the light source. DLP 3D printing usually use UV light or visible light, while SLA 3D printing utilizes a laser to happen the photopolymerization process. Another key difference is the mirror system. A digital micromirror device (DMD) is used in DLP 3D printing, while a galvanometer together with X–Y scanning mirror are utilized in SLA 3D printing. DMD is composed of an array of micrometer-sized mirrors which can rotate individually based on the designed pattern to regulate the light towards the liquid photopolymer. However, X–Y scanning mirror can only rotate as one single part to reflect the light direction with the help of galvanometers. Furthermore, DLP 3D printing uses a projector screen to project the structure of one layer to the liquid resin, leading to the photopolymerization process of all points simultaneously, while SLA 3D printing requires adjustments on the location of laser spot to cure all points on one layer (Fig. 10E and F), resulting in more time-consuming but better resolution performance. Both the methods are non-contact 3D printing, which provides a bunch of advantages, including being nozzle-free, no restriction on ink viscosity and high efficiency [129].

4.1.1. Digital light processing (DLP) 3D printing

Fantino et al. introduced a novel approach to fabricate 3D printed hydrogels with excellent mechanical and electrical properties. DLP 3D printing was used to fabricate PEGDA with a UV light intensity of 30 mW cm^{-2} and an X–Y resolution of 39 μm was achieved [126]. 3D printed PEGDA was then immersed into pyrrole solution for interfacial polymerization (Fig. 11a-d). Wales et al. fabricated a poly (ionic liquids) structure by employing DLP 3D printing [130]. Two different Ionic Liquids, [3-butyl-1-vinylimidazolium][dicyanamide] ([BVIM][N(CN)2]) and [3-butyl-1-vinylimidazolium][bis(trifluoromethane)sulfonimide] ([BVIM][NTf2]), were used and the synthesis processes employed exposure to an OSRAM lamp of 210 W. Thickness of each layer was 50 μm and exposed to the light for 8s to be polymerized. However, the high intensity of UV light would result in cell damage. Therefore, visible light has been considered as a more biofriendly source for DLP 3D printing [128]. Fu et al. used eosin Y as a photoinitiator for the photopolymerization of PEG and heparin under visible light exposure [131]. Heparin concentration (1.6–3.3% w/v), light intensity (5–100 mW cm^{-2} with a wavelength of 525 ± 15 nm) and gelation time (30–600s) were modified to obtain hydrogels with optimal properties. Cell viability evaluated with 3T3 fibroblast cells were found to be over 96%, indicating the advantage of using visible light for tissue engineering applications.

4.1.2. Stereolithography apparatus (SLA)

Heo et al. developed a photo-crosslinkable conductive hydrogel with high electrical conductivity [7]. PEDOT:PSS and PEGDA are mixed as a photocurable base for SLA 3D printing with a UV laser wavelength of 355 nm, 20 mJ intensity at 15 kHz. The printed constructs maintained structural integrity and had a conductivity range of 0.824×10^{-2} to 1.383×10^{-2} S/cm. Dorsal root ganglion neuronal cells (DRGs) were seeded in the printed structure, the live/dead assay demonstrated that the conductive hydrogel can maintain excellent cell viability and has no

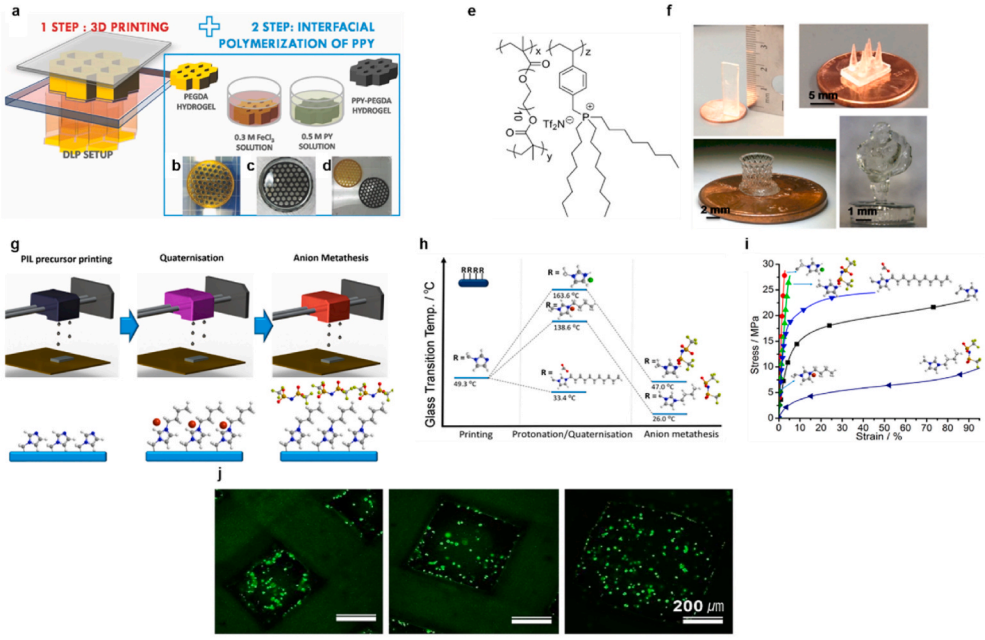

Fig. 11. (a) Schematic diagram of the 3D printing process. (b) DLP printed PEGDA structure. (c) PEGDA structure soaked in PY/CYH solution. (d) 3D printed PEGDA (color: yellow) and 3D printed PEGDA/PPY (color: black) structures [126]. (e) Molecular structure of poly(PEGDMA-co-TOPTf2N). (f) Mask projection microstereolithography printed 33 mm tall rectangular test specimens, 8 mm tall multi-cones, 8 mm tall grooved hyperboloid, and 8 mm tall figurine, respectively. Reprinted (adapted) with permission from (A. R. Schultz, P. M. Lambert, N. A. Chartrain, D. M. Ruohoniemi, Z. Zhang, C. Jangu, M. Zhang, C. B. Williams and T. E. Long, ACS Macro Letters, 2014, 3, 1205–1209.). Copyright (2014) American Chemical Society [18]. (g) Schematic illustration of the method used to both inkjet print polymerizable ionic liquids structure and post-printing functionalization process. (h) Variation of glass transition temperature of the film 2–40 along with the post-printing processes. (i) Stress−strain curves of the modified films. Reprinted (adapted) with permission from (E. Karjalainen, D. J. Wales, D. H. A. T. Gunasekera, J. Dupont, P. Licence, R. D. Wildman and V. Sans, ACS Sustainable Chemistry and Engineering, 2018, 6, 3984–3991.). Copyright (2018) American Chemical Society [19]. (j) Live/dead assay of encapsulated- DRG cells in GelMA with 3D printed PEDOT/PSS hydrogel on day 1. Reprinted from Materials Science and Engineering: C, Vol. 99, Dong Nyoung Heo,Se-Jun Lee, Raju Timsina, Xiangyun Qiu, Nathan J. Castro, Lijie Grace Zhang, Development of 3D printable conductive hydrogel with crystallized PEDOT:PSS for neural tissue engineering, Pages 582–590., Copyright (2019), with permission from Elsevier [7]. (For interpretation of the references to color in this figure legend, the reader is referred to the Web version of this article.)

remarkable cytotoxicity (Fig. 11j). Furthermore, accelerated differentiation of encapsulated DRGs was observed on applying electrical stimulation, indicating the potential of this approach in neural repair. Schultz et al. reported a microSLA 3D printing process for a ionic liquid network [18]. 4-vinylbenzyl trioctyl phosphonium bis(trifluoromethanesulfonate)imide (TOPTf2N) ionic liquid is used as one component to polymerize with two photocurable monomers, which are 1,4-butanediol diacrylate (BDA) and poly(ethylene glycol) dimethacrylate (PEGDMA) (Fig. 11e,f), respectively. The advantages of this process include using a low UV intensity of 5 mW cm^{-2} and a high digital resolution less than 10 um.

4.2. Inkjet bioprinting

Inkjet bioprinting is derived from inkjet printing, by the substitution of normal ink cartridges with cell-laden bioink cartridges. Inkjet bioprinting has a high resolution (around 50 μm) and a high printing speed with limitations on high viscosity materials and nozzle clogging problems [3]. Based on the releasing mechanism of nozzle, inkjet bioprinting can be divided into two groups, which are continuous inkjet printing and drop-on-demand inkjet printing [3]. Continuous inkjet printing can provide an uninterrupted bioinks stream on the platform, while drop-on-demand inkjet printing can release the droplets one by one on demand [132]. Drop-on-demand inkjet printing allows precise control and high efficiency to construct complex structures of tissues and organs. Karjalainen et al. used drop-on-demand inkjet printing to fabricate polymerizable ionic liquids structure [19]. In this study, 1-vinylimidazole (Vilm), butyl acrylate (BuA) and divinylbenzene (DVB) were successfully cross-linked by UV photopolymerization using 2-hydroxy-2-methylpropiophenone (HMP) as the initiator. Post-printing functionalization including quaternization, protonation and anion metathesis were applied to modify the mechanical properties (glass transition temperature, yield stress) of the printed films (Fig. 11g-i). During post-polymerization processes, printed films were covalently modified by various reagents (HCl, bis(trifluoromethane) sulfonimide (NTf2), dodecanoic acid, etc.) to modify the mechanical properties. The successful post-polymerization process provided a huge degree of freedom to control the mechanical properties of 3D printed poly ionic liquid films. Vijayavenkataraman et al. developed a customized electrohydrodynamic jetting (EHD-jet) 3D bioprinter to fabricate scaffolds with high resolution (5 μm aligned fibers) and low operation voltage (2–3 kV) [133]. Different from conventional inkjet 3D printing, in which the droplet size is constrained by the nozzle diameter, EHD-jet is regarded as a solution to produce small droplets without the necessity of decreasing the nozzle diameter due to the large “neck-down” ratio between the nozzle diameter and jet diameter [134,135]. PPy block PCL and PCL/rGO scaffolds were successfully fabricated by EHD-jet printing, while exhibiting higher cell growth rate and better cell differentiation [117,118].

4.3. Extrusion-based bioprinting

Among all the 3D printing technologies that have been applied to tissue engineering area, extrusion based bioprinting is the most commonly used method [136]. The bioink is stored in the cartridges and dispensed through nozzles by pneumatic pressure, piston or screw mechanism (Fig. 10D). Bioinks for extrusion bioprinting must satisfy a number of requirements including shear thinning property, shape fidelity, and cell viability, directly relating to its printability [137]. Low viscosity bioink would result in less control and low resolution, while high viscosity would require a high extrusion force, leading to cell damage and death. Proper viscosities of bioinks for extrusion-based bioprinting vary between 30 and 6×10^7 mPa s [138]. Viscosity of shear thinning material decreases as the shear rate increases, leading to a smooth extrusion of bioink through the nozzle and hence expected of a bioink used in extrusion bioprinting. Spencer et al. developed a novel

method to use extrusion-based printing to directly print a mixture of GelMA and PEDOT:PSS into a complicated, cell-laden 3D structure [4]. They found that the viscosity of bioinks continuously decrease as the temperature decreases and the viscosity at room temperature (25 °C) is too low to provide a stable structure. A biocompatible support bath maintained at 4 °C to ensure proper bioink viscosity was introduced and the nozzle directly printed the structures within the bath. On encapsulating C2C12 myoblasts into the bioinks (printed with a 160um diameter nozzle), the post-printing cell viability was over 95%. The shear-thinning property of GelMA/PEDOT: PSS inks protect the cells from being damaged by the shear stress, thus maintaining high cell viability. This work demonstrated that the drawbacks of extrusion-based bioprinting could be partially compensated with the help of a support bath and used for fabrication of complicated cell-laden structures. The addition of conductive block co-polymer of PCL and PPy to collagen improved the printability of the hydrogel compared to pure collagen and the *in vitro* studies proved the biocompatibility of the collagen/PPy-b-PCL bioink [139]. Ma et al. combined extrusion-based 3D printing and solvent casting to produce a poly-L-lactide/PPy based 2D film with uniform thickness and no bubbles [140]. On the basis of mechanical and cytocompatibility test results, adequate mechanical properties were achieved by adjusting the PPy concentration and cell viability was maintained to be higher than 80% all the time. The potential capability to fabricate both 2D and 3D scaffolds via extrusion-based printing method can lead to a wide range of applications in tissue engineering. Another challenge is the limited resolution of extrusion-based bioprinting. Compared to other bioprinting methods, extrusion-based bioprinting has the lowest resolution (roughly 100 μm) [3]. Decreasing the diameter of nozzle could enhance the resolution, but will be detrimental to the cells as the shear rate would increase with decreasing nozzle diameter [141].

Table 4 summarizes the published works on bioprinting of printing various conductive materials.

5. Biomedical applications of 3D-printed conductive materials

Owing to the adequate repeatability, easy operation, biocompatibility and high conductivity, 3D printed conductive materials have gained therapeutic attractions for different applications including engineered tissues/organs and biosensors. Given the growing population of aged people and technological advancements, the possibilities of irreversible tissue injuries are set to increase. The development of

Table 4
Summary of bioprinted conductive materials.

Material	Printing method	Printing support	Printing resolution	Properties	Biocompatibility	Ref.
PEGDA and PPY	DLP 3D Printing	UV light with 30 mW cm^{-2}	X–Y resolution of 39 μm	Electrically conductive and mechanically tough	–	[126]
[BVIM][N(CN)2] and [BVIM][NTf2]	DLP 3D Printing	OSRAM lamp of 210 W for 8s	50 mm/layer	–	–	[130]
PEG and heparin	DLP 3D Printing	Visible light with an intensity of 5–100 mW cm^{-2} and a wavelength of 525 ± 15 nm	–	Able to deliver growth factors, safer than UV light	3T3 fibroblast cells are seeded with cell viability more than 96%	[131]
PEDOT:PSS and PEGDA	SLA 3D Printing	UV laser with 355 nm wavelength and 20 μJ intensity at 15 kHz	–	Conductivity varies from 0.824×10^{-2} to 1.383×10^{-2} S/cm	DRG cells shows excellent cell viability when seeded on the surface of the hydrogel	[7]
TOPTf2N and BDA; TOPTf2N and PEGDMA	Micro stereolithography 3D printing	UV intensity of 5 mW cm^{-2}	Less than 10 μm	High thermal stability and ion conductivity	–	[18]
GelMA and PEDOT:PSS	Extrusion-based bioprinting printing	Constant temperature support bath at 4 °C	120–140 μm	Shear-thinning property	Encapsulated C2C12 myoblasts with cell viability over 95%	[4]
Vilm and BuA	drop-on-demand inkjet printing	UV induced photopolymerization process	5 μm/layer	Allows post polymerization processes to adjust the mechanical properties of 3D printed film	–	[19]
decellularized adipose tissue encapsulates human adipose tissue-derived mesenchymal stem cells (hASCs)	Extrusion-based bioprinting	Pneumatic pressure is in 20 kPa for extrusion	–	compressive modulus is 122.56 ± 20.23 kPa. Increase the expression of standard adipogenic genes	hASCs cell viability over 80% at day 14	[142]
PEGDA, polyacrylamide (PAAm)	DLP 3D printing	405 nm light emitting diode (LED) projector	150 μm in X–Y dimentions	Young's Modulus: 0.01 MPa; Compressive modulus: 435.4 ± 17.7 kPa (maximum); Elastic modulus: more than 156 kPa; average sheet resistance: 231.0 Ω/sq to 222.5 Ω/sq	–	[143]
PANI	Inkjet printing	Sequentially printing two different solutions onto the substrate and allowing the polymerization process happen on the substrate	–	Electrical conductivity was 0.23 S/cm at room temperature	–	[144]
Collagen, PPy-block-poly (caprolactone)	Extrusion-based bioprinting	Using syringe pump to inject the bioink	–	Conductivity was in the order of 1–5 × 10^{-3} S/cm	PC12 cells were capsulated in the hydrogel and maintained excellent cell viability	[145]
GelMA, PANI	Micro stereolithography 3D printing	UV intensity of 25 mW cm^{-2} for 10 s	–	Impedance of 9 ± 0.3 kΩ	10T1/2 cells were cultured and exhibited similar response on cell adhesion and cell viability	[146]

conductive 3D printed artificial tissues and organs is expected to promote the regeneration process by enhanced cell-cell communication and better integrate with the natural electrical potential in human body [147]. Furthermore, conductive material integrated biosensors target highly-sensitive, accurate and rapid detection of human metabolites for screening, diagnosis, and patient monitoring [148].

5.1. Nerve scaffold

Nerve injuries, including central nerve injury and peripheral nerve injury, refers to destruction, damage or crushing of the nerve leading to severe sensory or motor impairment [149,150]. External treatments are required to facilitate the regeneration process when the nerve experiences a complete transection and fails to re-establish sufficient nerve functions. Commonly used clinical methods including direct coaptation, autograft and allograft suffer from non-suitability for large nerve gap injuries, donor site morbidity, and donor site availability [151]. These constraints often impede the widespread application of these methods and restoration of complete neurological function becomes challenging. Therefore, by applying customized structures, conductive materials and stimulus methods, nerve guidance conduits have increasingly become crucial for nerve regeneration. Furthermore, the inclusion of conductive materials allows the application of external electrical stimulus through various methods (direct coupling, capacitive coupling, inductive) [23]. By giving a proper electrical stimulus, different cell behaviors can be promoted via the activation of certain signal pathways and ion channels, therefore improving the axon regeneration performance [152,153]. Zhu et al. illustrated that neural stem cells proliferation and differentiation can be promoted by the integration between carbon nanofibrous scaffolds and biphasic electrical stimulation [55]. Lee et al. developed a conductive mesh by deploying PPy on electrospun poly (lactic-co-glycolic acid) (PLGA) nanofibers [154]. PPY-PLGA structure was examined to be non-toxic and supportive for PC12 cell proliferation and differentiation. With an external electrical field of 10 mV/cm, PC12 cells were found to achieve 40–50% longer neurites and 40–90% more neurite quantities compared to regeneration performance without electrical stimulations. Vijayavenkataraman et al. fabricated a novel conductive scaffold made of PCL and Poly(acrylic acid) (PAA) [155]. The result further proved that PC12 cells proliferation and differentiation were improved by the use of conductive material. Furthermore, controllable variation of both mechanical properties and biodegradability by adjusting the concentration ratio between PCL and PAA prove its potential to be used as guidance conduits to treat nerve injuries.

5.2. Cardiovascular tissues

In the past few decades, cardiovascular disease (CVD) had become one of the leading causes of death worldwide, killing more than 17.9 million people each year with more than half of the deaths attributed to people above 70 years old [156,157]. As the population ages, the magnitude of high-risk group will increase, leading to the ever-growing demand for cardiovascular tissue regeneration and transplantation. As human cardiomyocytes possess a restricted regeneration capacity and the formation of scar tissue could further limit the cardiac contractile capacity to defunctionalize the damaged cardiovascular tissue, the cardiac damage could be a permanent process and cause the heart death [158]. Heart transplantation has been proved to be an effective surgical transplant procedure targets to failure cardiovascular tissues, however the large-scale application is constrained by donor availability and potential rejection reactions. In the recent years, cardiovascular tissue engineering has been intensively explored to pave the way for the construction of functional cardiovascular scaffolds. Since electrical impulses are crucial to maintain the systemic circulation through synchronized contraction and blood pumping, the integration of conductive material in cardiovascular scaffolds has been an emerging area of research to realize a better functional restoration of the cardiovascular system [159,160]. Martins et al. dispersed carbon nanofibers into chitosan matrix to form a highly conductive composite for cardiac tissue engineering [161]. The carbon nanofibers/chitosan scaffold supported cardiac cell attachment, proliferation and enhanced the restoration of cardiogenic properties while maintaining similar mechanical properties compared with the native cardiac muscle. Shin et al. found that the deployment of CNT/GelMA scaffold contributes to better cardiomyocytes proliferation and differentiation [162]. Furthermore, the existence of CNTs protected the cardiac tissue from being damaged by doxorubicin and heptanol, which are cardio toxic and cardio inhibitor respectively. Mooney et al. excited the differentiation of MSC into cardiomyocyte lineage by the use of electroactive CNT as a substrate to transfer the electrical stimulation [49]. Cardiac markers were detected through qPCR method and the differentiation related proteins were stained and observed after electrical stimulation.

5.3. Other biomedical applications

Conductive material has been widely used in tissue engineering to assist the recovery of damaged tissues and other biomedical applications, including biosensors to detect certain biomolecules, actuator for artificial muscles, probe DNA orientation binding for higher sensitivity and electron exchange, etc [163].

The concentration of human metabolites (glucose, uric acid, cholesterol, etc.) closely relates to the human health and a human metabolites disorder can cause severe health problems [164,165]. For the current clinical method, it remains a challenge to construct a biosensor that is integrated in a single chip with highly sensitive multi-metabolites detection capacity [166]. The combination of nanotechnology, biology and material science enables the development of multifunctional biosensing nanodevices. Li et al. developed a low-cost and biocompatible platinum nanoparticle embedded polyaniline hydrogel based biosensor that can simultaneously detect all types of metabolites with high sensitivity and rapid response time [167]. The hierarchical porosity structure of polyaniline hydrogel enhances the molecular permeability, and particularly, the excellent electronic conductivity increases the electron transfer rate. Owing to those unique features, the multifunctional biosensor exhibits high sensitivity for a wide range of various metabolites concentration (uric acid, cholesterol, etc.). The detection range can be further expanded by focusing on a single biomolecule with the assistance of conductive materials. Zhai et al. introduced a glucose enzyme sensor made by platinum nanoparticles-polyaniline hydrogel with high sensitivity and wide detection range [168]. Normally, glucose needs to be converted into gluconolactone, leading to the formation of hydrogen peroxide, which is used as an indicator to detect the glucose level in human body [169,170]. The hybrid biosensor utilizes porosity structure of polyaniline hydrogel, allowing the immobilization of enzymes, and catalytic function of platinum nanoparticles to decompose the hydrogen peroxide, which is produced during the enzymatic reaction. The electrochemical signals can then be efficiently collected by the biosensor, benefitting from the high conductivity platinum nanoparticle-based polyaniline hydrogels with fast response time (3s), wide linear range (0.01–8 mM) and low detection limit (0.7 μM).

The change of volume of conductive materials during electrochemical reaction allows the application as actuators in artificial muscle movements. Furthermore, the volumetric deformation level is determined by the magnitude of the applied voltage [171]. Based on the dimension of involved anions, the electrochemical reaction and conductive material deformation direction can be classified into cation drive and anion drive processes. Small anion can lead to a shrinkage of the conductive material results from reduction process by anion drive. Large anion can result in swollen conductive materials via cation drive due to the entanglement and immobilization of long alkyl chains in the structure network [172,173]. The bending direction of conductive material-based actuators can then be controlled by certain driven methods. Garcia-Cordova et al. developed a triple layer actuator

fabricated by the polypyrrole and dodecylbenzenesulfonate to achieve simultaneous actuating and sensing procedures in a single device [174]. Conductive polymer is chosen due to the low operation voltage, which is regarded as a more cost-efficient option. After immersing the actuator into the electrolyte, a uniform bending direction was achieved owing to two different driven methods happened on two opposite layers (anion-driven swelling on one layer and cation-driven shrinking on the other layer).

Genetic science experienced a rapid development during the past two decades, thanks to the identification of disease related DNA sequences through polymerase chain reaction method. Conductive material embedded DNA biosensors possesses the capability to detect specific DNA sequence via the redox signal when target DNA binds with probe DNA [163]. CNT-incorporated biosensor (also called genosensors) has gained significant appeal by promoting sequential binding of the probe DNA and increasing the detection sensitivity. Zhang et al. introduced both zinc oxide nanoparticles and MWCNTs to construct a novel conductive DNA biosensor that was meant to detect phosphinothricin acetyltransferase gene in transgenic corn [175]. The wide detection range (from 1.0 × 10–11 to 1.0 × 10-6 mol/L) and low detection limit (2.8 × 10–12 mol/L) pave the way for a lot other conductive material-embedded DNA biosensor applications.

6. Conclusion and future perspective

A comprehensive overview of different conductive materials, associated 3D fabrication methods and corresponding biomedical applications utilizing a proper electrical stimulation owing to the high conductivities were presented in detail. Conductive materials have been widely examined and developed for various biomedical applications over the past few decades. An ideal conductive material should be highly conductive, biocompatible, biodegradable and non-cytotoxic with suitable mechanical properties and structural integrity. PPY, PANI and PEDOT: PSS are the three most commonly used intrinsic conductive polymers, while graphene, CNT, metal nanoparticles, and ionic liquids are considered as significant filler composites to tune both the electrical and mechanical properties of the synthesized conductive materials. ILs has a huge potential to be explored for tissue engineering applications, given the massive choices, excellent ionic conductivity, and the ability to tune both electrical and mechanical properties of the polymer composites by modulating the choice and composition of ILs.

Furthermore, the induction of conductive materials into scaffolds can enhance the electric transfer rate and efficiency across the scaffolds, therefore resulting in a significant improvement of various cell behaviors, such as cell alignment, cell migration, cell proliferation and cell differentiation, by providing a proper electrical stimulus. Electrical stimulation intensity and duration are critical parameters to be considered that has a large effect on tissue repair and regeneration. Thanks to the excellent conductivity and biocompatibility, conductive materials had been proved to be a strong candidate for the fabrication of nerve and cardiovascular tissues as both of those tissues require potential transfer to maintain the physiological function. In biosensors, conventional biosensors suffer from slow response, confined detection range and single type molecule detection, which allows the integration of conductive material as a promising method to fabricate a highly sensitive multifunctional biosensor. Due to the volumetric change upon electrochemical reaction, conductive materials can be utilized to construct biocompatible actuators for artificial muscles.

However, there still remains some limitations before fully utilizing conductive materials in clinical and hospital applications, including low biodegradability of nanoparticles, brittle mechanical properties of polypyrrole and polyaniline, etc. Nevertheless, massive efforts have been taken to examine various methods to resolve those constraints. As a response to low biodegradable conductive materials, attempts have been made to mix biodegradable materials, including poly(lactic-co-glycolic acid) and poly(L-lactic acid), with non-biodegradable conductive materials in an effort to achieve an adequate degradation rate through the degradation of the backbone of the crosslinked structure. Owing to the rapid development of 3D printing technology, structural integrity and mechanical properties can be tuned by adjusting the CAD model, printing parameters as well as using different printing methods. Depending on the type of bioprinting, the properties of conductive bioinks required varies. For light-based bioprinting, the bioinks must be photo-polymerizable while for extrusion and inkjet bioprinting, the viscosities of the bioinks must be optimized.

Recent advances in 3D printing and bioprinting of conductive materials indicate the huge potential of these materials in engineered tissues and organs. Regeneration performance has been proved to undergo a significant improvement both *in vitro* and *in vivo* owing to the advantages of biomimetic potential transfer, promoted cell behaviors and similar mechanical properties compared with the native tissue. However, considering the lack of knowledge on the molecular mechanisms of cell differentiation due to the inherent material conductivity and external electrical stimulation, a robust and comprehensive evaluation of all the potential risks is required before attempting clinical trials [176]. In spite of that, the combination of electrical stimulation, conductive biomaterials, and 3D bioprinting would have a synergistic effect on fabricating tissues with better biomimicry, that would significantly accelerate the tissue repair, regeneration and integration with the host tissue.

Declaration of competing interest

The authors declare that they have no known competing financial interests or personal relationships that could have appeared to influence the work reported in this paper.

References

[1] L.G. Griffith, G. Naughton, Tissue engineering - current challenges and expanding opportunities, Science 295 (5557) (2002), 1009-1010+1012-1014.
[2] P. Zarrintaj, et al., Conductive biomaterials as nerve conduits: recent advances and future challenges, Appl. Mater. Today 20 (2020).
[3] S. Vijayavenkataraman, et al., 3D bioprinting of tissues and organs for regenerative medicine, Adv. Drug Deliv. Rev. 132 (2018) 296–332.
[4] A.R. Spencer, et al., Bioprinting of a cell-laden conductive hydrogel composite, ACS Appl. Mater. Interfaces 11 (34) (2019) 30518–30533.
[5] D. Radenkovic, A. Solouk, A. Seifalian, Personalized development of human organs using 3D printing technology, Med. Hypotheses 87 (2016) 30–33.
[6] R.K. Pal, et al., Mechanically robust, photopatternable conductive hydrogel composites, React. Funct. Polym. 120 (2017) 66–73.
[7] D.N. Heo, et al., Development of 3D printable conductive hydrogel with crystallized PEDOT:PSS for neural tissue engineering, Mater. Sci. Eng. C 99 (2019) 582–590.
[8] X. Liu, et al., Functionalized carbon nanotube and graphene oxide embedded electrically conductive hydrogel synergistically stimulates nerve cell differentiation, ACS Appl. Mater. Interfaces 9 (17) (2017) 14677–14690.
[9] X. Xiao, et al., Preparation and property evaluation of conductive hydrogel using poly (vinyl alcohol)/polyethylene glycol/graphene oxide for human electrocardiogram acquisition, Polymers 9 (12) (2017).
[10] P. Baei, et al., Electrically conductive gold nanoparticle-chitosan thermosensitive hydrogels for cardiac tissue engineering, Mater. Sci. Eng. C 63 (2016) 131–141.
[11] I. Noshadi, et al., Engineering biodegradable and biocompatible bio-ionic liquid conjugated hydrogels with tunable conductivity and mechanical properties, Sci. Rep. 7 (1) (2017) 4345.
[12] Y.S. Kim, et al., Highly conductive and hydrated PEG-based hydrogels for the potential application of a tissue engineering scaffold, React. Funct. Polym. 109 (2016) 15–22.
[13] M. Yamada, et al., Electrical stimulation modulates fate determination of differentiating embryonic stem cells, Stem Cell. 25 (3) (2007) 562–570.
[14] Y. Bu, et al., A conductive sodium alginate and carboxymethyl chitosan hydrogel doped with polypyrrole for peripheral nerve regeneration, RSC Adv. 8 (20) (2018) 10806–10817.
[15] G. Kaur, et al., Electrically conductive polymers and composites for biomedical applications, RSC Adv. 5 (47) (2015) 37553–37567.
[16] A. Navaei, et al., Electrically conductive hydrogel-based micro-topographies for the development of organized cardiac tissues, RSC Adv. 7 (6) (2017) 3302–3312.
[17] W.C. Yan, et al., 3D bioprinting of skin tissue: from pre-processing to final product evaluation, Adv. Drug Deliv. Rev. 132 (2018) 270–295.
[18] A.R. Schultz, et al., 3D printing phosphonium ionic liquid networks with mask projection microstereolithography, ACS Macro Lett. 3 (11) (2014) 1205–1209.

[19] E. Karjalainen, et al., Tunable ionic control of polymeric films for inkjet based 3D printing, ACS Sustain. Chem. Eng. 6 (3) (2018) 3984–3991.
[20] L. Di Silvio, 15 - bone tissue engineering and biomineralization, in: A. R. Boccaccini, J.E. Gough (Eds.), Tissue Engineering Using Ceramics and Polymers, Woodhead Publishing, 2007, pp. 319–331.
[21] D. Albulet, et al., Chapter 1 - nanotechnology for personalized medicine: cancer research, diagnosis, and therapy, in: A. Ficai, A.M. Grumezescu (Eds.), Nanostructures for Cancer Therapy, Elsevier, 2017, pp. 1–21.
[22] R.E. McClelland, et al., Chapter 6 - tissue engineering, in: J.D. Enderle, J. D. Bronzino (Eds.), Introduction to Biomedical Engineering, third ed., Academic Press, Boston, 2012, pp. 273–357.
[23] C. Chen, et al., Electrical stimulation as a novel tool for regulating cell behavior in tissue engineering, Biomater. Res. 23 (1) (2019).
[24] R. Nuccitelli, et al., Nanosecond pulsed electric field stimulation of reactive oxygen species in human pancreatic cancer cells is Ca2+-dependent, Biochem. Biophys. Res. Commun. 435 (4) (2013) 580–585.
[25] N. Tandon, et al., Alignment and elongation of human adipose-derived stem cells in response to direct-current electrical stimulation, in: Proceedings of the 31st Annual International Conference of the IEEE Engineering in Medicine and Biology Society: Engineering the Future of Biomedicine, EMBC 2009, 2009.
[26] K.E. Hammerick, M.T. Longaker, F.B. Prinz, In vitro effects of direct current electric fields on adipose-derived stromal cells, Biochem. Biophys. Res. Commun. 397 (1) (2010) 12–17.
[27] M. Radisic, et al., Functional assembly of engineered myocardium by electrical stimulation of cardiac myocytes cultured on scaffolds, Proc. Natl. Acad. Sci. U. S. A 101 (52) (2004) 18129–18134.
[28] K.R. Robinson, The responses of cells to electrical fields: a review, JCB (J. Cell Biol.) 101 (6) (1985) 2023–2027.
[29] G. Yang, et al., Regulation of adipose-tissue-derived stromal cell orientation and motility in 2D- and 3D-cultures by direct-current electrical field, Dev. Growth Differ. 59 (2) (2017) 70–82.
[30] Z. Zhao, et al., Directing migration of endothelial progenitor cells with applied DC electric fields, Stem Cell Res. 8 (1) (2012) 38–48.
[31] S.J. Bunn, A. Lai, J. Li, DC electric fields induce perpendicular alignment and enhanced migration in schwann cell cultures, Ann. Biomed. Eng. 47 (7) (2019) 1584–1595.
[32] R. Tzoneva, Influence of electric field on cell behavior. Electrotreatment of cells for biomedical applications, Asian J. Phys. 23 (2014) 789–814.
[33] J.F. Feng, et al., Brief report: guided migration of neural stem cells derived from human embryonic stem cells by an electric field, Stem Cell. 30 (2) (2012) 349–355.
[34] S.N. Iwasa, et al., Charge-balanced electrical stimulation can modulate neural precursor cell migration in the presence of endogenous electric fields in mouse brains, eNeuro 6 (6) (2019).
[35] C.L. Ross, The use of electric, magnetic, and electromagnetic field for directed cell migration and adhesion in regenerative medicine, Biotechnol. Prog. 33 (1) (2017) 5–16.
[36] L. Yao, et al., Exploration of molecular pathways mediating electric field-directed schwann cell migration by RNA-seq, J. Cell. Physiol. 230 (7) (2015) 1515–1524.
[37] P.K. Mattila, P. Lappalainen, Filopodia: molecular architecture and cellular functions, Nat. Rev. Mol. Cell Biol. 9 (6) (2008) 446–454.
[38] F.C. Tsai, et al., Ca2+ signaling in cytoskeletal reorganization, cell migration, and cancer metastasis, BioMed Res. Int. 2015 (2015).
[39] J. Zhang, et al., Electrically guiding migration of human induced pluripotent stem cells, Stem Cell Rev. Rep. 7 (4) (2011) 987–996.
[40] L. Yao, et al., Small applied electric fields guide migration of hippocampal neurons, J. Cell. Physiol. 216 (2) (2008) 527–535.
[41] V. Mironova, J. Xu, A single-cell view of tissue regeneration in plants, Curr. Opin. Plant Biol. 52 (2019) 149–154.
[42] J. Sun, G. Nan, The extracellular signal-regulated kinase 1/2 pathway in neurological diseases: a potential therapeutic target (Review), Int. J. Mol. Med. 39 (6) (2017) 1338–1346.
[43] P. Dong, Explore Rb/E2F Activation Dynamics to Define the Control Logic of Cell Cycle Entry in Single Cells, 2015.
[44] H. Durgam, et al., Novel degradable co-polymers of polypyrrole support cell proliferation and enhance neurite out-growth with electrical stimulation, J. Biomater. Sci. Polym. Ed. 21 (10) (2010) 1265–1282.
[45] B. Sun, et al., Polypyrrole-coated poly(l-lactic acid-: Co -ε-caprolactone)/silk fibroin nanofibrous membranes promoting neural cell proliferation and differentiation with electrical stimulation, J. Mater. Chem. B 4 (41) (2016) 6670–6679.
[46] S. Iwanami, S. Iwami, Quantitative immunology by data analysis using mathematical models, in: S. Ranganathan, et al. (Eds.), Encyclopedia of Bioinformatics and Computational Biology, Academic Press, Oxford, 2019, pp. 984–992.
[47] F. Pires, et al., Neural stem cell differentiation by electrical stimulation using a cross-linked PEDOT substrate: expanding the use of biocompatible conjugated conductive polymers for neural tissue engineering, Biochim. Biophys. Acta Gen. Subj. 1850 (6) (2015) 1158–1168.
[48] X. Liu, et al., Electrical stimulation promotes nerve cell differentiation on polypyrrole/poly (2-methoxy-5 aniline sulfonic acid) composites, J. Neural. Eng. 6 (6) (2009).
[49] E. Mooney, et al., The electrical stimulation of carbon nanotubes to provide a cardiomimetic cue to MSCs, Biomaterials 33 (26) (2012) 6132–6139.
[50] X. Yuan, et al., Electrical stimulation enhances cell migration and integrative repair in the meniscus, Sci. Rep. 4 (2015).
[51] N.J. Gunja, et al., Migration responses of outer and inner meniscus cells to applied direct current electric fields, J. Orthop. Res. 30 (1) (2012) 103–111.
[52] U.H. Ko, et al., Promotion of myogenic maturation by timely application of electric field along the topographical alignment, Tissue Eng. 24 (9–10) (2018) 752–760.
[53] N. Özkucur, et al., Local calcium elevation and cell elongation initiate guided motility in electrically stimulated osteoblast-like cells, PloS One 4 (7) (2009).
[54] H. Hayashi, et al., The effect of pulsed electric fields on the electrotactic migration of human neural progenitor cells through the involvement of intracellular calcium signaling, Brain Res. 1652 (2016) 195–203.
[55] W. Zhu, et al., Enhanced neural stem cell functions in conductive annealed carbon nanofibrous scaffolds with electrical stimulation, Nanomed. Nanotechnol. Biol. Med. 14 (7) (2018) 2485–2494.
[56] B. Kapeller, et al., Microcurrent stimulation promotes reverse remodelling in cardiomyocytes, ESC Heart Failure 3 (2) (2016) 122–130.
[57] A. Llucià-Valldeperas, et al., Electrical stimulation of cardiac adipose tissue-derived progenitor cells modulates cell phenotype and genetic machinery, J. Tissue Eng. Regen. Med. 9 (11) (2015) E76–E83.
[58] J. Liu, et al., Highly conductive hydrogel polymer fibers toward promising wearable thermoelectric energy harvesting, ACS Appl. Mater. Interfaces 10 (50) (2018) 44033–44040.
[59] M. Hameed, Magnetic conductive hydrogel nanocomposites as drug carrier, Nanosci. Nanotechnol. (2016) 48–58.
[60] M.R.J. MacDiarmid Alan Graham, R.B. Kaner, Porter Lord, The concept of 'doping' of conducting polymers: the role of reduction potentials, Philos. Trans. R. Soc. A 314 (1528) (1985) 3–15.
[61] Z. Ma, et al., Doping engineering of conductive polymer hydrogels and their application in advanced sensor technologies, Chem. Sci. 10 (25) (2019) 6232–6244.
[62] U. Lange, N.V. Roznyatovskaya, V.M. Mirsky, Conducting polymers in chemical sensors and arrays, Anal. Chim. Acta 614 (1) (2008) 1–26.
[63] J. Shabani Shayeh, et al., Conductive polymer/reduced graphene oxide/Au nano particles as efficient composite materials in electrochemical supercapacitors, Appl. Surf. Sci. 353 (2015) 594–599.
[64] S.I. Na, et al., Efficient and flexible ITO-free organic solar cells using highly conductive polymer anodes, Adv. Mater. 20 (21) (2008) 4061–4067.
[65] D. Naegele, R. Bittihn, Electrically conductive polymers as rechargeable battery electrodes, Solid State Ionics 28–30 (1988) 983–989.
[66] Z.B. Huang, et al., Conducting polypyrrole in tissue engineering applications, Front. Mater. Sci. 8 (1) (2014) 39–45.
[67] A. Peramo, et al., In situ polymerization of a conductive polymer in acellular muscle tissue constructs, Tissue Eng. 14 (3) (2008) 423–432.
[68] A.D. Bendrea, L. Cianga, I. Cianga, Review paper: progress in the field of conducting polymers for tissue engineering applications, J. Biomater. Appl. 26 (1) (2011) 3–84.
[69] Q. Wu, et al., A robust, highly stretchable supramolecular polymer conductive hydrogel with self-healability and thermo-processability, Sci. Rep. 7 (1) (2017).
[70] Z. Wang, et al., Ultrastretchable strain sensors and arrays with high sensitivity and linearity based on super tough conductive hydrogels, Chem. Mater. 30 (21) (2018) 8062–8069.
[71] M. Satoh, et al., Temperature dependence of mechanical properties of electrochemically prepared polypyrole film, Synth. Met. 20 (1) (1987) 79–83.
[72] L. Dai, Intelligent Macromolecules for Smart Devices : from Materials Synthesis to Device Applications, Springer-Verlag, London, 2010.
[73] K. Deshmukh, et al., Biopolymer composites with high dielectric performance: interface engineering, in: Biopolymer Composites in Electronics, 2017, pp. 27–128.
[74] E.J. Oh, et al., Polyaniline: dependency of selected properties on molecular weight, Synth. Met. 55 (2–3) (1993) 977–982.
[75] H. Valentová, J. Stejskal, Mechanical properties of polyaniline, Synth. Met. 160 (7–8) (2010) 832–834.
[76] Z. Bagher, et al., Conductive hydrogel based on chitosan-aniline pentamer/gelatin/agarose significantly promoted motor neuron-like cells differentiation of human olfactory ecto-mesenchymal stem cells, Mater. Sci. Eng. C 101 (2019) 243–253.
[77] U. Lang, J. Dual, Mechanical properties of the intrinsically conductive polymer poly(3,4-ethylenedioxythiophene) poly(styrenesulfonate) (PEDOT/PSS), in: Key Engineering Materials, 2007, pp. 1189–1192.
[78] B.J. Worfolk, et al., Ultrahigh electrical conductivity in solution-sheared polymeric transparent films, Proc. Natl. Acad. Sci. U. S. A 112 (46) (2015) 14138–14143.
[79] J. Cameron, P.J. Skabara, The damaging effects of the acidity in PEDOT:PSS on semiconductor device performance and solutions based on non-acidic alternatives, Mater. Horizons 7 (7) (2020) 1759–1772.
[80] J.M. Wessels, et al., Optical and electrical properties of three-dimensional interlinked gold nanoparticle assemblies, J. Am. Chem. Soc. 126 (10) (2004) 3349–3356.
[81] D. Untereker, et al., Maximum conductivity of packed nanoparticles and their polymer composites, ACS Appl. Mater. Interfaces 1 (1) (2009) 97–101.
[82] C.Z. Yuan, et al., Hierarchically structured carbon-based composites: design, synthesis and their application in electrochemical capacitors, Nanoscale 3 (2) (2011) 529–545.
[83] K. Tadyszak, J.K. Wychowaniec, J. Litowczenko, Biomedical applications of graphene-based structures, Nanomaterials 8 (11) (2018).
[84] J. Zhu, et al., The application of graphene in lithium ion battery electrode materials, SpringerPlus 3 (1) (2014).

[85] S. Stankovich, et al., Graphene-based composite materials, Nature 442 (7100) (2006) 282–286.
[86] C. Lee, et al., Measurement of the elastic properties and intrinsic strength of monolayer graphene, Science 321 (5887) (2008) 385–388.
[87] S. Chuah, et al., Nano reinforced cement and concrete composites and new perspective from graphene oxide, Construct. Build. Mater. 73 (2014) 113–124.
[88] X.F. Zhang, S. Gurunathan, Biofabrication of a novel biomolecule-assisted reduced graphene oxide: an excellent biocompatible nanomaterial, Int. J. Nanomed. 11 (2016) 6635–6649.
[89] B.D. Holt, A.M. Arnold, S.A. Sydlik, In it for the long haul: the cytocompatibility of aged graphene oxide and its degradation products, Adv. Healthc. Mater. 5 (23) (2016) 3056–3066.
[90] L. Han, et al., A mussel-inspired conductive, self-adhesive, and self-healable tough hydrogel as cell stimulators and implantable bioelectronics, Small 13 (2) (2017).
[91] Y. Zhu, et al., Graphene and graphene oxide: synthesis, properties, and applications, Adv. Mater. 22 (35) (2010) 3906–3924.
[92] D.A. Dikin, et al., Preparation and characterization of graphene oxide paper, Nature 448 (7152) (2007) 457–460.
[93] L. Qiu, et al., Dispersing carbon nanotubes with graphene oxide in water and synergistic effects between graphene derivatives, Chem. Eur J. 16 (35) (2010) 10653–10658.
[94] D.R. Dreyer, et al., The chemistry of graphene oxide, Chem. Soc. Rev. 39 (1) (2010) 228–240.
[95] P. Kalluru, et al., Nano-graphene oxide-mediated in vivo fluorescence imaging and bimodal photodynamic and photothermal destruction of tumors, Biomaterials 95 (2016) 1–10.
[96] R. Rudra, et al., Graphite oxide incorporated crosslinked polyvinyl alcohol and sulfonated styrene nanocomposite membrane as separating barrier in single chambered microbial fuel cell, J. Power Sources 341 (2017) 285–293.
[97] C. Cheng, et al., Biopolymer functionalized reduced graphene oxide with enhanced biocompatibility via mussel inspired coatings/anchors, J. Mater. Chem. B 1 (3) (2013) 265–275.
[98] S.R. Shin, et al., Reduced graphene oxide-GelMA hybrid hydrogels as scaffolds for cardiac tissue engineering, Small 12 (27) (2016) 3677–3689.
[99] A.M. Holban, A.M. Grumezescu, E. Andronescu, Inorganic nanoarchitectonics designed for drug delivery and anti-infective surfaces, in: Surface Chemistry of Nanobiomaterials: Applications of Nanobiomaterials, 2016, pp. 301–327.
[100] R.B. Rakhi, Preparation and properties of manipulated carbon nanotube composites and applications, in: Nanocarbon and its Composites: Preparation, Properties and Applications, 2018, pp. 489–520.
[101] L. Mottet, et al., A conductive hydrogel based on alginate and carbon nanotubes for probing microbial electroactivity, Soft Matter 14 (8) (2018) 1434–1441.
[102] E. Piñón-Segundo, N. Mendoza-Muñoz, D. Quintanar-Guerrero, Chapter 23 - nanoparticles as dental drug-delivery systems, in: K. Subramani, W. Ahmed, J. K. Hartsfield (Eds.), Nanobiomaterials in Clinical Dentistry, William Andrew Publishing, 2013, pp. 475–495.
[103] T.R. Correia, et al., 3D Printed scaffolds with bactericidal activity aimed for bone tissue regeneration, Int. J. Biol. Macromol. 93 (2016) 1432–1445.
[104] H. Chen, et al., Magnetic cell-scaffold interface constructed by superparamagnetic IONP enhanced osteogenesis of adipose-derived stem cells, ACS Appl. Mater. Interfaces 10 (51) (2018) 44279–44289.
[105] P. Zhang, et al., Electrospun doping of carbon nanotubes and platinum nanoparticles into the β-phase polyvinylidene difluoride nanofibrous membrane for biosensor and catalysis applications, ACS Appl. Mater. Interfaces 6 (10) (2014) 7563–7571.
[106] M.R. Das, et al., Synthesis of silver nanoparticles in an aqueous suspension of graphene oxide sheets and its antimicrobial activity, Colloids Surf. B Biointerfaces 83 (1) (2011) 16–22.
[107] D.V. Gopinath, et al., Biosynthesis of silver nanoparticles from Tribulus terrestris and its Antimicrobial activity: a novel biological approach, Colloids Surf. B Biointerfaces (2012).
[108] K. Zhu, et al., Gold nanocomposite bioink for printing 3D cardiac constructs, Adv. Funct. Mater. 27 (12) (2017).
[109] L. Li, et al., All inkjet-printed amperometric multiplexed biosensors based on nanostructured conductive hydrogel electrodes, Nano Lett. 18 (6) (2018) 3322–3327.
[110] Q. Zhao, J.L. Anderson, 2.11 - ionic liquids, in: J. Pawliszyn (Ed.), Comprehensive Sampling and Sample Preparation, Academic Press, Oxford, 2012, pp. 213–242.
[111] Y.-Y. Jiang, et al., SO2 gas separation using supported ionic liquid membranes, J. Phys. Chem. B 111 (19) (2007) 5058–5061.
[112] J.M. Gomes, S.S. Silva, R.L. Reis, Biocompatible ionic liquids: fundamental behaviours and applications, Chem. Soc. Rev. 48 (15) (2019) 4317–4335.
[113] K. Roy, S. Kar, R.N. Das, Chapter 12 - future avenues, in: K. Roy, S. Kar, R.N. Das (Eds.), Understanding the Basics of QSAR for Applications in Pharmaceutical Sciences and Risk Assessment, Academic Press, Boston, 2015, pp. 455–462.
[114] C.W. Whang, J.F. Jen, P.V. Kumar, 3.32 - recent advances in solid-phase microextraction for environmental applications, in: J. Pawliszyn (Ed.), Comprehensive Sampling and Sample Preparation, Academic Press, Oxford, 2012, pp. 629–656.
[115] J.I. Santos, et al., Environmental safety of cholinium-based ionic liquids: assessing structure-ecotoxicity relationships, Green Chem. 17 (9) (2015) 4657–4668.
[116] M. Petkovic, et al., Novel biocompatible cholinium-based ionic liquids—toxicity and biodegradability, Green Chem. 12 (4) (2010) 643–664.
[117] S. Vijayavenkataraman, et al., 3D-Printed PCL/rGO conductive scaffolds for peripheral nerve injury repair, Artif. Organs 43 (5) (2019) 515–523.
[118] S. Vijayavenkataraman, et al., 3D-Printed PCL/PPy conductive scaffolds as three-dimensional porous nerve guide conduits (NGCs) for peripheral nerve injury repair, Front. Bioeng. Biotechnol. 7 (2019).
[119] J. Lin, et al., The synthesis and electrical conductivity of a polyacrylate/graphite hydrogel, React. Funct. Polym. 67 (4) (2007) 275–281.
[120] H. Nulwala, A. Mirjafari, X. Zhou, Ionic liquids and poly(ionic liquid)s for 3D printing – a focused mini-review, Eur. Polym. J. 108 (2018) 390–398.
[121] D. Kazmer, 28 - three-dimensional printing of plastics, in: M. Kutz (Ed.), Applied Plastics Engineering Handbook, second ed., William Andrew Publishing, 2017, pp. 617–634.
[122] W.K. Durfee, P.A. Iaizzo, Chapter 21 - medical applications of 3D printing, in: P. A. Iaizzo (Ed.), Engineering in Medicine, Academic Press, 2019, pp. 527–543.
[123] S. Chameettachal, F. Pati, 12 - polymeric gels for tissue engineering applications, in: K. Pal, I. Banerjee (Eds.), Polymeric Gels, Woodhead Publishing, 2018, pp. 305–330.
[124] R.D. Pedde, et al., Emerging biofabrication strategies for engineering complex tissue constructs, Adv. Mater. 29 (19) (2017) 1606061.
[125] P. Soman, et al., Digital microfabrication of user-defined 3D microstructures in cell-laden hydrogels, Biotechnol. Bioeng. 110 (11) (2013) 3038–3047.
[126] E. Fantino, et al., 3D printing/interfacial polymerization coupling for the fabrication of conductive hydrogel, Macromol. Mater. Eng. 303 (4) (2018) 1700356.
[127] J. Lee, et al., Effect of degree of crosslinking and polymerization of 3D printable polymer/ionic liquid composites on performance of stretchable piezoresistive sensors, Smart Mater. Struct. 26 (3) (2017).
[128] Z. Zheng, et al., Visible light-induced 3D bioprinting technologies and corresponding bioink materials for tissue engineering: a review, Engineering (2020).
[129] P.N. Bernal, et al., Volumetric bioprinting of complex living-tissue constructs within seconds, Adv. Mater. 31 (42) (2019).
[130] D.J. Wales, et al., 3D-Printable photochromic molecular materials for reversible information storage, Adv. Mater. 30 (26) (2018).
[131] A. Fu, et al., Visible-light-initiated thiol-acrylate photopolymerization of heparin-based hydrogels, Biomacromolecules 16 (2) (2015) 497–506.
[132] S. Iwanaga, K. Arai, M. Nakamura, Chapter 4 - inkjet bioprinting, in: A. Atala, J. J. Yoo (Eds.), Essentials of 3D Biofabrication and Translation, Academic Press, Boston, 2015, pp. 61–79.
[133] S. Vijayavenkataraman, et al., Electrohydrodynamic-jetting (EHD-jet) 3D-printed functionally graded scaffolds for tissue engineering applications, J. Mater. Res. 33 (14) (2018) 1999–2011.
[134] D. Gao, J.G. Zhou, Designs and applications of electrohydrodynamic 3D printing, Int. J. Bioprinting 5 (1) (2019).
[135] D. Gao, et al., Mechanisms and modeling of electrohydrodynamic phenomena, Int. J. Bioprinting 5 (1) (2019).
[136] S.C. Lee, et al., Physical and chemical factors influencing the printability of hydrogel-based extrusion bioinks, Chem. Rev. 120 (19) (2020) 10834–10886.
[137] D.M. Kirchmajer, R. Gorkin Iii, M. In Het Panhuis, An overview of the suitability of hydrogel-forming polymers for extrusion-based 3D-printing, J. Mater. Chem. B 3 (20) (2015) 4105–4117.
[138] K.A. Deo, et al., Bioprinting 101: design, fabrication, and evaluation of cell-laden 3D bioprinted scaffolds, Tissue Eng. 26 (5–6) (2020) 318–338.
[139] S. Vijayavenkataraman, et al., Conductive collagen/polypyrrole-b-polycaprolactone hydrogel for bioprinting of neural tissue constructs, Int. J. Bioprinting 5 (2.1) (2019).
[140] C. Ma, et al., 3D printing of conductive tissue engineering scaffolds containing polypyrrole nanoparticles with different morphologies and concentrations, Materials 12 (15) (2019).
[141] R. Chang, J. Nam, W. Sun, Effects of dispensing pressure and nozzle diameter on cell survival from solid freeform fabrication-based direct cell writing, Tissue Eng. 14 (1) (2008) 41–48.
[142] F. Pati, et al., Biomimetic 3D tissue printing for soft tissue regeneration, Biomaterials 62 (2015) 164–175.
[143] X.Y. Yin, et al., 3D printing of ionic conductors for high-sensitivity wearable sensors, Mater. Horizons 6 (4) (2019) 767–780.
[144] L. Pan, et al., Hierarchical nanostructured conducting polymer hydrogel with high electrochemical activity, Proc. Natl. Acad. Sci. Unit. States Am. 109 (24) (2012) 9287.
[145] S. Vijayavenkataraman, et al., Conductive collagen/polypyrrole-b-polycaprolactone hydrogel for bioprinting of neural tissue constructs, Int. J. Bioprinting 5 (2.1) (2019) 31–43. Special Issue.
[146] Y. Wu, et al., Fabrication of conductive gelatin methacrylate–polyaniline hydrogels, Acta Biomater. 33 (2016) 122–130.
[147] M.L. Hernández-Bule, M.Á. Trillo, A. Úbeda, Molecular mechanisms underlying antiproliferative and differentiating responses of hepatocarcinoma cells to subthermal electric stimulation, PloS One 9 (1) (2014).
[148] Cyclodextrins based electrochemical sensors for biomedical and pharmaceutical analysis, Curr. Med. Chem. 24 (22) (2017) 2359–2391.
[149] Z.P. Aguilar, Chapter 6 - nanomedical devices, in: Z.P. Aguilar (Ed.), Nanomaterials for Medical Applications, Elsevier, 2013, pp. 235–292.
[150] S.S. Soman, S. Vijayavenkataraman, Perspectives on 3d bioprinting of peripheral nerve conduits, Int. J. Mol. Sci. 21 (16) (2020) 5792.
[151] D. Cinteza, et al., Peripheral nerve regeneration - an appraisal of the current treatment options, Maedica 10 (1) (2015) 65–68.
[152] Q. Liu, B. Song, Electric field regulated signaling pathways, Int. J. Biochem. Cell Biol. 55 (2014) 264–268.

[153] S.S. Soman, S. Vijayavenkataraman, Applications of 3D bioprinted-induced pluripotent stem cells in healthcare, Int. J. Bioprinting 6 (4) (2020).
[154] J.Y. Lee, et al., Polypyrrole-coated electrospun PLGA nanofibers for neural tissue applications, Biomaterials 30 (26) (2009) 4325–4335.
[155] S. Vijayavenkataraman, et al., Electrohydrodynamic jet 3D-printed PCL/PAA conductive scaffolds with tunable biodegradability as nerve guide conduits (NGCs) for peripheral nerve injury repair, Mater. Des. 162 (2019) 171–184.
[156] L. Kiraly, S. Vijayavenkataraman, Biofabrication in congenital cardiac surgery: a plea from the operating theatre, promise from science, Micromachines 12 (3) (2021) 332.
[157] F. Quadri, S.S. Soman, S. Vijayavenkataraman, Progress in Cardiovascular Bioprinting, Artificial Organs, 2021.
[158] M.L. Steinhauser, R.T. Lee, Regeneration of the heart, EMBO Mol. Med. 3 (12) (2011) 701–712.
[159] S. Ahadian, A. Khademhosseini, Smart scaffolds in tissue regeneration, Regen. Biomater. 5 (3) (2018) 125–128.
[160] M. Montgomery, et al., Flexible shape-memory scaffold for minimally invasive delivery of functional tissues, Nat. Mater. 16 (10) (2017) 1038–1046.
[161] A.M. Martins, et al., Electrically conductive chitosan/carbon scaffolds for cardiac tissue engineering, Biomacromolecules 15 (2) (2014) 635–643.
[162] Su Ryon Shin, S.M. J, Momen Zalabany, Keekyoung Kim, Pinar Zorlutuna, Sang bok Kim, M.K. Mehdi Nikkhah, Azize Mohamed, Jing Kong, Kai-tak Wan, Tomas Palacios, H.B. Mehmet, R. Dokmeci, Xiaowu (Shirley) Tang, Ali Khademhosseini, Carbon-nanotube-embedded hydrogel sheets for engineering cardiac constructs and bioactuators, ACS Nano 7 (2013) 2369–2380.
[163] C.B. Jacobs, M.J. Peairs, B.J. Venton, Review: carbon nanotube based electrochemical sensors for biomolecules, Anal. Chim. Acta 662 (2) (2010) 105–127.
[164] J. Wang, Electrochemical glucose biosensors, Chem. Rev. 108 (2) (2008) 814–825.
[165] M. Gerard, A. Chaubey, B.D. Malhotra, Application of conducting polymers to biosensors, Biosens. Bioelectron. 17 (5) (2002) 345–359.
[166] Y. Zhao, et al., 3D nanostructured conductive polymer hydrogels for high-performance electrochemical devices, Energy Environ. Sci. 6 (10) (2013) 2856–2870.
[167] L. Li, et al., A nanostructured conductive hydrogels-based biosensor platform for human metabolite detection, Nano Lett. 15 (2) (2015) 1146–1151.
[168] D. Zhai, et al., Highly sensitive glucose sensor based on pt nanoparticle/polyaniline hydrogel heterostructures, ACS Nano 7 (4) (2013) 3540–3546.
[169] Z.F. Li, et al., Covalent immobilization of glucose oxidase on the surface of polyaniline films graft copolymerized with acrylic acid, Biomaterials 19 (1–3) (1998) 45–53.
[170] H. Kim, et al., Immobilization of glucose oxidase into polyaniline nanofiber matrix for biofuel cell applications, Biosens. Bioelectron. 26 (9) (2011) 3908–3913.
[171] Y. Park, J. Jung, M. Chang, Research progress on conducting polymer-based biomedical applications, Appl. Sci. 9 (6) (2019).
[172] T.F. Otero, J.J. Sanchez, J.G. Martinez, Biomimetic dual sensing-actuators based on conducting polymers. Galvanostatic theoretical model for actuators sensing temperature, J. Phys. Chem. B 116 (17) (2012) 5279–5290.
[173] K. Asaka, H. Okuzaki, Soft actuators: materials, modeling, applications, and future perspectives, Soft Actuators: Mater. Model. Appl. Future Perspect. 9784431547679 (2014) 1–507.
[174] F. García-Córdova, et al., Biomimetic polypyrrole based all three-in-one triple layer sensing actuators exchanging cations, J. Mater. Chem. 21 (43) (2011) 17265–17272.
[175] W. Zhang, et al., Synergistic effects of nano-ZnO/multi-walled carbon nanotubes/chitosan nanocomposite membrane for the sensitive detection of sequence-specific of PAT gene and PCR amplification of NOS gene, J. Membr. Sci. 325 (1) (2008) 245–251.
[176] S. Vijayavenkataraman, A perspective on bioprinting ethics, Artif. Organs (2016) 1033–1038.